

# Fundamental Limits for Location and Velocity Estimation using Signals of Opportunity

Mei Leng, Wee Peng Tay, Chong Meng Samson See, Sirajudeen Gulam Razul, and  
Moe Z. Win

## Abstract

We consider the problem of localizing two sensors using signals of opportunity from beacons with known positions. Beacons and sensors have asynchronous local clocks or oscillators with unknown clock skews and offsets. We model clock skews as random, and analyze the biases introduced by clock asynchronism in the received signals. By deriving the equivalent Fisher information matrix for the modified Bayesian Cramér-Rao lower bound (CRLB) of sensor position and velocity estimation, we quantify the errors caused by clock asynchronism. We propose an algorithm based on differential time-difference-of-arrival and frequency-difference-of-arrival that mitigates the effects of clock asynchronism to estimate the sensor positions and velocities. Simulation results suggest that our proposed algorithm is robust and approaches the CRLB when clock skews have small standard deviations.

## Index Terms

Signals of opportunity, asynchronous clocks, localization, DTDOA.

M. Leng and W.P. Tay are with the Nanyang Technological University, Singapore. (e-mail: {lengmei,wptay}@ntu.edu.sg).

C.M. Samson See and S.G. Razul are with TL@NTU, Singapore. (e-mail: samsonsee,ESirajudeen@ntu.edu.sg).

Moe Z. Win is with the Laboratory for Information and Decision Systems (LIDS), Massachusetts Institute of Technology (e-mail: moewin@mit.edu).

This research is supported by the DRTech-TL@NTU grant TL-9010100261-04.

## I. INTRODUCTION

Ubiquitous computing and location-aware services necessitate the development of localization methods for mobile sensors or devices. For example, detection and inference using wireless sensor networks [1]–[3] require sensor locations to meaningfully interpret the collected data, and mobile positions are indispensable for location based services. A common localization method is the use of the Global Positioning System (GPS). However, GPS signals are generally limited to areas with a clear sky view, and do not penetrate well through obstacles, which makes it impractical for use in indoor and urban environments. Alternatives to GPS localization have been widely investigated, with methods using signals of opportunity (SOOP) attracting much interest recently [4]–[8]. The SOOP are public signals transmitted for various non-localization applications, including AM/FM radio signals, digital television signals, cellular communication signals, and WiFi signals. These signals conform to well-established standards and can be easily detected in most urban areas. We call their transmitters beacons and their locations are usually known a priori.

Localization using SOOP is based on signal metrics like received-signal-strength (RSS), angle-of-arrival (AOA), time-difference-of-arrival (TDOA) and frequency-difference-of-arrival (FDOA). Algorithms using TDOA and/or FDOA measurements are robust against multi-path effects, and do not require knowledge of the signal transmission time or waveforms. These methods typically assume that the clocks of beacons and sensors are synchronized (see [6], [9] and references therein). Clock synchronization is however difficult to achieve and maintain in practice [10], [11]. In some cases, beacons such as GSM base stations, are “passive” transmitters, and cannot synchronize with the sensors. Furthermore, unlike GPS signals that are generated by satellite atomic oscillators with extremely small skews (less than  $10^{-11}$ , [12]), SOOP are usually generated by beacons with less perfect oscillators that have clock skews as large as  $10^{-4}$  [13], and clock offsets as large as  $10^{-3}$ . Therefore, it is of interest to investigate the effect of asynchronous clocks on localization accuracy.

Source localization algorithms using a set of asynchronous static sensors were proposed in [14] and [15]. The source is assumed to emit a sequence of short pulses, and each pulse has a period that can be measured by a known number of clock ticks. TDOA measurements are made by counting the number of received pulses, which requires specially designed pulse waveforms. A more general case

was investigated in [16] where all beacons and sensors have asynchronous clocks. They assume that each sensor knows the beacons' transmitted waveforms so that the time-of-arrival (TOA) of a beacon signal can be estimated locally. The TDOA between two sensors is then obtained by subtracting one TOA from another, and the authors do not consider errors introduced by communication and sampling.

In this paper, we investigate the localization and velocity estimation of moving sensors using arbitrary narrowband SOOP. We assume that sensors know the nominal carrier frequencies of the beacons but have no knowledge of their waveforms. We also assume that each sensor or beacon has a local oscillator that controls its clock, and we use the terms clock and oscillator interchangeably. We are interested to quantify the fundamental performance limit of sensor location and velocity estimation in the presence of clock asynchronism, and to develop estimation algorithms that mitigate its effects. Our main contributions are the following.

- We analyze the biases introduced by asynchronous clocks in the beacons and sensors, and derive expressions for the received signals at each sensor (cf. Theorem 1). We show that the time and frequency offsets in the received signals are corrupted by beacon and sensor clock offsets and skews. Our analysis includes the scenario studied in [16] as a special case.
- We derive the fundamental limits for sensor location and velocity estimation using SOOP from asynchronous beacons (cf. Theorem 2). The CRLB for localization and tracking have been extensively studied in the literature, but most works are based on the statistical characteristics of signal metrics like TDOA and FDOA [17]. As pointed out in [18], signal metrics depend heavily on the specific measurement method, which may discard useful information during processing. We treat the sensor clock skews as nuisance random variables, and we derive an approximate equivalent Fisher information matrix (EFIM) associated with the modified Bayesian CRLB for sensor locations and velocities, directly from the received signals. We show that the approximate EFIM does not depend on sensor and beacon clock offsets, which suggests that there exists estimation procedures that does not require a priori knowledge of these quantities.
- We propose a location estimation algorithm based on the differences between multiple TDOA

TABLE I  
COMMONLY USED NOTATIONS

Notations	Definition
$\mathcal{S}, \mathcal{B}$	set of sensors and beacons, respectively
$\beta_m, \Omega_m$	clock skew and clock offset of $m \in \mathcal{S} \cup \mathcal{B}$ , respectively
$\mathcal{T}_{j,b}, \mathcal{D}_{j,b}$	propagation delay and nominal Doppler shift from beacon $b$ to sensor $j$ , respectively
$\mathbf{u}_{j,b}, \mathbf{w}_{j,b}$	direction vectors between sensor $j$ and beacon $b$ defined in (3) and (10), respectively
$\hat{\tau}_b, \hat{\xi}_b$	TDOA and FDOA estimates respectively at $S_1$ using signals of beacon $b$
$\mathbf{F}_x$	Fisher information matrix (FIM) of the modified Bayesian CRLB for $\mathbf{x}$
$\mathbf{F}_{e,s}$	equivalent Fisher information matrix (EFIM) for sensor location and velocity estimates
$P_b, W_b, T_b$	energy, RMS bandwidth, and RMS integration time of the signal transmitted from beacon $b$ , respectively
$\lambda_b, \epsilon_b$	constants related to beacon $b$ 's signal characteristics and defined in (17)

estimates, which we call differential TDOA (DTDOA) [16]. Sensor velocities are then estimated based on the position estimates and the FDOA. Simulation results suggest that our proposed algorithm is robust to clock asynchronism, and achieves a root mean squared error (RMSE) close to the CRLB when the standard deviations of sensor clock skews are smaller than  $10^{-2}$ .

The rest of this paper is organized as follows. In Section II, we present the system model. In Section III, we derive the Fisher information matrix for the modified Bayesian CRLB based on the received signals at each sensor. In Section IV, we obtain closed-form expressions for TDOA and FDOA estimates, and we propose an algorithm for location and velocity estimation. In Section V, we present numerical results and we conclude in Section VI. For the reader's ease of reference, we summarize some commonly used notations in Table I.

## II. SYSTEM MODEL

We consider the problem of localizing two sensors using signals from a set  $\mathcal{B}$  of  $N$  beacons. An example scenario is shown in Figure 1. The beacon  $b \in \mathcal{B}$  has a known fixed position  $\mathbf{p}_b$ , and it broadcasts a narrowband signal at a nominal carrier frequency  $f_b$ . Two sensors,  $S_1$  and  $S_2$  are at unknown locations  $\mathbf{p}_1$  and  $\mathbf{p}_2$ , and moving with unknown velocities  $\mathbf{v}_1$  and  $\mathbf{v}_2$  respectively. Denote the set of sensors as  $\mathcal{S} = \{1, 2\}$ . Our goal is to estimate the locations  $\mathbf{p}_j$  and velocities  $\mathbf{v}_j$  for  $j \in \mathcal{S}$ , using SOOP from the beacons.

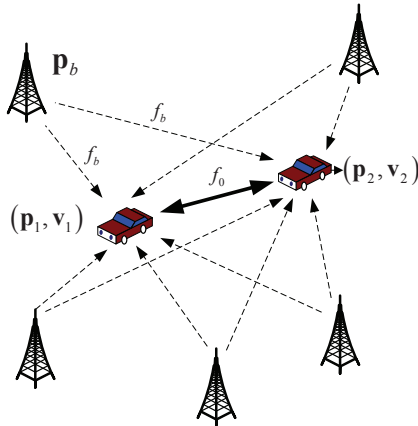


Fig. 1. Using signals from beacons to estimate sensor locations and velocities.

We suppose that each beacon  $b$  has a local oscillator operating with clock skew  $\beta_b$  and clock offset  $\Omega_b$ , so that its local time  $t_b(t)$  with respect to (w.r.t.) a universal standard time  $t$  is given by [19]

$$t_b(t) = \beta_b t + \Omega_b. \quad (1)$$

The clock skew  $\beta_b$  characterizes the clock drift rate and the clock offset  $\Omega_b$  characterizes any clock errors and clock drifts accumulated up to time  $t$ . We approximate the clock offset  $\Omega_b$  to be constant over our observation period, and its value generally ranges from  $-10\text{ms}$  to  $10\text{ms}$  [13]. Similarly, each sensor  $j$  has a local oscillator with local time given by  $t_j(t) = \beta_j t + \Omega_j$ .

The rate at which an oscillator drifts depends on various random quantities like its quality, power level, temperature and other environmental variables. Since clock skew is non-negative, we assume that sensor and beacon clock skews are independent Gamma random variables with mean 1 and standard deviation  $\sigma_{\beta_m}$ , for  $m \in \mathcal{S} \cup \mathcal{B}$ . We also assume that these random variables do not depend on the beacon or sensor positions and velocities. The expected value of clock skews is assumed to be 1 because clocks generally drift slowly w.r.t. the standard time and its standard deviation  $\sigma_{\beta_m}$  varies between  $10^{-6}$  and  $10^{-3}$  [13], [20]. It will be obvious later that our analysis is easily generalizable to other distributions [21] as long as the quantities  $\mathbb{E}\{1/\beta_m\}$  and  $\mathbb{E}\{1/\beta_m^2\}$  exist and are finite.

We assume that each sensor has no prior knowledge of the signal waveform transmitted by beacons. However, sensors know the *nominal* carrier frequencies used by the beacons and the

positions of the beacons. We also assume that signals from different beacons can be distinguished at sensors. Sensors forward its received signals to each other by communicating over a wireless channel with nominal passband frequency  $f_0$ . To perform self-localization, each sensor obtains TDOA and FDOA measurements by cross-correlating signals received by itself and by the other sensor. Since local signal processing, including signal generation and sampling, depends on the local oscillator, the TDOA and FDOA measurements obtained at each sensor will be distorted by their asynchronous oscillators. In the following, we first analyze how such distortions affect the transmitted and received signals, and then derive closed-form expressions for TDOA and FDOA based on the distorted signals.

#### A. Delays and Doppler Shifts

In this section, we briefly describe the wireless channel for communications between beacons and sensors. We assume that every wireless channel has a flat fading time-varying impulse response. For each  $b \in \mathcal{B}$ , and each sensor  $S_j$ ,  $j \in \mathcal{S}$ , we suppose that the channel between  $b$  and  $S_j$  have an impulse response  $h_{j,b}(t) = \alpha_{j,b}\delta(t - \tau_{j,b}(t))$  [22]. Let the propagation delay between  $b$  and  $S_j$  be

$$\mathcal{T}_{j,b} = \frac{\|\mathbf{p}_j - \mathbf{p}_b\|}{c}, \quad (2)$$

where  $c$  is the speed of light, and let the nominal Doppler shift observed at  $S_j$  be

$$\mathcal{D}_{j,b} = -\frac{f_b}{c} \mathbf{v}_j^T \underbrace{\frac{\mathbf{p}_j - \mathbf{p}_b}{\|\mathbf{p}_j - \mathbf{p}_b\|}}_{\triangleq \mathbf{u}_{j,b}}, \quad (3)$$

where  $\mathbf{u}_{j,b}$  is the normalized direction from  $S_j$  to beacon  $b$ . We approximate the propagation time from  $b$  to  $S_j$  as  $\tau_{j,b}(t) \approx \mathcal{T}_{j,b} - \mathcal{D}_{j,b}t/f_b$ , and hence the impulse response is given by  $h_{j,b}(t) = \alpha_{j,b}\delta(\gamma_{j,b}t - \mathcal{T}_{j,b})$ , where  $\gamma_{j,b} = 1 + \mathcal{D}_{j,b}/f_b$ .

Similarly, the impulse response of the channel from sensor  $S_2$  to sensor  $S_1$  is given by  $h_{1,2}(t) = \alpha_{1,2}\delta(\gamma_{1,2}t - \mathcal{T}_{1,2})$ , where  $\mathcal{T}_{1,2} = \|\mathbf{p}_1 - \mathbf{p}_2\|/c$  is the propagation delay between the sensors, and  $\mathcal{D}_{1,2} = -f_0(\mathbf{v}_1 - \mathbf{v}_2)^T \mathbf{u}_{1,2}/c$  is the Doppler shift observed at sensor  $S_1$ , and  $\gamma_{1,2} = 1 + \mathcal{D}_{1,2}/f_0$ .

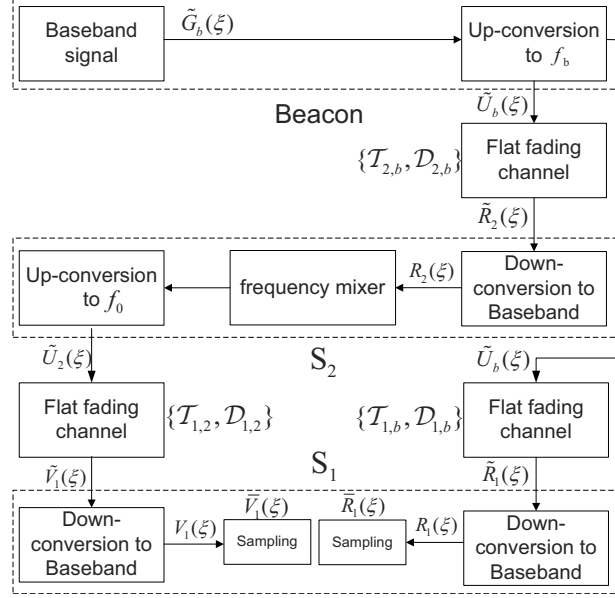


Fig. 2. Block diagram for communications between beacons and sensors.

### B. Received Signals at Sensors

Suppose that beacon  $b$  generates a nominal baseband signal  $g_b(t)$ . Because of clock skew and offset at the beacon, the actual baseband signal is  $\tilde{g}_b(t) = g_b(\beta_b t + \Omega_b)$ , which is then up-converted to the nominal passband frequency  $f_b$  at the beacon for transmission, and the actual passband frequency may differ from  $f_b$  due to the clock skew of beacon  $b$ . Since we do not assume that sensors know the nominal baseband signal  $g_b(t)$  used by the beacon, it suffices to consider only the signal  $\tilde{g}_b(t)$ . However, to make the connections with TOA methods and scenarios where  $g_b(t)$  is a known pilot signal clear, we have chosen to explicitly characterize signals in terms of  $g_b(t)$  (cf. Remarks 1 and 2 later). Let  $G_b(\xi)$  be the Fourier transform of  $g_b(t)$ .

The sensor  $S_1$  receives the signal from beacon  $b$ , and then performs demodulation and sampling (see Figure 2). Each step involves signal processing using the local oscillator, which introduces errors due to its clock skew and offset. We derive the signal at each processing step in Proposition 1, whose proof is given in Appendix A. Let  $i = \sqrt{-1}$ .

**Proposition 1** *Suppose that beacon  $b \in \mathcal{B}$  transmits a signal with baseband representation  $\tilde{G}_b(\xi)$  to sensor  $S_j$  over a flat fading channel. We have the following.*

(i) At beacon  $b$ , the baseband signal  $\tilde{g}_b(t)$  has positive frequency part

$$\tilde{G}_b(\xi) = \frac{1}{\beta_b} G_b(\xi/\beta_b) \exp\{i2\pi\xi\Omega_b/\beta_b\}.$$

(ii) At beacon  $b$ , the transmitted passband signal  $\tilde{u}_b(t)$  has positive frequency part

$$\tilde{U}_b(\xi) = \tilde{G}_b(\xi - f_b\beta_b) \exp\{i2\pi f_b\Omega_b\}.$$

(iii) At  $S_j$ , the passband signal received from beacon  $b$ ,  $\tilde{r}_{j,b}(t)$ , has positive frequency part

$$\tilde{R}_{j,b}(\xi) = \frac{1}{\gamma_{j,b}} \tilde{U}_b(\xi/\gamma_{j,b}) \exp\{-i2\pi\xi\mathcal{T}_{j,b}/\gamma_{j,b}\}.$$

(iv) At  $S_j$ , the signal after down conversion to baseband,  $r_{j,b}(t)$ , has positive frequency part

$$R_{j,b}(\xi) = \tilde{R}_{j,b}(\xi + f_b\beta_j) \exp\{-i2\pi f_b\Omega_j\}.$$

(v) Suppose  $S_j$  samples the received signal at Nyquist rate of  $1/T$  so that the sampling impulse train is  $\sum_{n=-\infty}^{+\infty} \delta(\beta_j t - nT)$ . The sampled signal has positive frequency part  $R_{j,b}(\beta_j\xi)$ .

Sensor  $S_1$  utilizes both its own received signal and that received by sensor  $S_2$  to obtain TDOA and FDOA measurements. In practice, sensor  $S_2$  forwards its received signal to  $S_1$  by first doing a frequency translation to passband  $f_0$  and then transmitting through the wireless channel  $h_{1,2}(t) = \alpha_{1,2}\delta(\gamma_{1,2}t - \mathcal{T}_{1,2})$  (cf. Figure 2). The received signals at sensor  $S_1$  after sampling is given in Theorem 1, whose proof is provided in Appendix B.

**Theorem 1** Let  $g_b(t)$  be the nominal baseband signal to be generated by beacon  $b$ , and  $G_b(\xi)$  be its Fourier transform. The received signal at sensor  $S_1$  from beacon  $b$  has baseband representation

$$R_{1,b}(\xi) \propto G_b[(\beta_1\xi - \Upsilon_{1,b})/(\beta_b\gamma_{1,b})] e^{-i2\pi\xi \frac{\beta_1\Delta_{1,b}}{\beta_b\gamma_{1,b}}}, \quad (4)$$

where  $\Delta_{1,b} = \mathcal{T}_{1,b}\beta_b - \Omega_1\beta_b/\beta_1 - \Omega_b$  and  $\Upsilon_{1,b} = f_b(\gamma_{1,b}\beta_b - \beta_1)$ . The received signal at sensor  $S_1$  from sensor  $S_2$  has baseband representation

$$V_{1,b}(\xi) \propto G_b[(\beta_1\xi - \Psi_{1,b})/(\beta_b\gamma_{1,2}\gamma_{2,b})] e^{-i2\pi\xi \frac{\beta_1\Lambda_{1,b}}{\beta_b\gamma_{1,2}\gamma_{2,b}}}, \quad (5)$$

where  $\Lambda_{1,b} = \mathcal{T}_{2,b}\beta_b + \mathcal{T}_{1,2}\gamma_{2,b}\beta_b - \Omega_2\beta_b/\beta_2 - \Omega_b$ , and  $\Psi_{1,b} = f_b\gamma_{1,2}(\gamma_{2,b}\beta_b - \beta_2) + f_0(\gamma_{1,2}\beta_2 - \beta_1)$ .

*Remark 1:* Suppose that sensors are static. When all beacon clocks are synchronized (i.e.,  $\beta_b = 1$  and  $\Omega_b = 0$  for  $b \in \mathcal{B}$ ), the received signal (4) reduces to that in [18]. Assuming further that the signal  $g_b(t)$  can be generated locally by sensor  $S_1$ , the TOA estimate obtained by cross-correlating  $r_{1,b}(t)$  and  $g_b(t)$  is given by  $\mathcal{T}_{1,b} - \Omega_1$  as in [18].

*Remark 2:* Suppose that sensors are static. The local TOA value at  $S_j$  in [16] is based on time-stamp values and is given by  $\mathcal{T}_{j,b}\beta_b - \Omega_1\beta_b/\beta_1 - \Omega_b$ , which equals to  $\Delta_{1,b}$  with  $\gamma_{1,b} = 1$  in Theorem 1. The TDOA between two sensors  $S_1$  and  $S_2$  in [16] is then given by direct subtraction as  $\Delta_{2,b} - \Delta_{1,b}$ .

### III. MODIFIED CRLB FOR LOCATION AND VELOCITY ESTIMATION

In this section, we derive the fundamental limits for location and velocity estimation using the received signals at  $S_1$ . Let  $T$  be the sampling interval, and  $T_{ob}$  be the total observation time. For each beacon  $b \in \mathcal{B}$ , let  $r_b[1 : T_{ob}/T]$  and  $v_b[1 : T_{ob}/T]$  be the sampled sequence of the received signal from  $b$  received at sensor  $S_1$ , and the signal from  $b$  retransmitted from  $S_2$  to  $S_1$ , respectively. Taking the inverse Fourier transform of (4) and (5), we have for each  $l = 1, \dots, T_{ob}/T$ ,

$$r_b[l] = \underbrace{g_b(\beta_b\gamma_{1,b}t/\beta_1 - \Delta_{1,b}) \exp\{-i2\pi\Upsilon_{1,b}t/\beta_1\}}_{\triangleq \mu_b[l]}|_{t=lT} + \varpi_b^r(t)|_{t=lT}, \quad (6)$$

$$v_b[l] = \underbrace{g_b(\beta_b\gamma_{1,2}\gamma_{2,b}t/\beta_1 - \Lambda_{1,b}) \exp\{-i2\pi\Psi_{1,b}t/\beta_1\}}_{\triangleq \theta_b[l]}|_{t=lT} + \varpi_b^v(t)|_{t=lT}. \quad (7)$$

The terms  $\varpi_b^r(t)$  and  $\varpi_b^v(t)$  in (6) and (7) are observation noises, modeled as additive complex white Gaussian processes with power spectral density  $P_0$ . We assume that all noise processes are independent. Let  $\mathbf{r} = \{r_b[1 : T_{ob}/T] : b \in \mathcal{B}\}$  and  $\mathbf{v} = \{v_b[1 : T_{ob}/T] : b \in \mathcal{B}\}$  be the collection of observations from all beacons.

Our analysis is based on the received sequences given by (6) and (7). Treating the sensor clock skews as nuisance parameters, there are  $4L + 2 + 2N$  unknown parameters  $\mathbf{p}_1, \mathbf{p}_2, \mathbf{v}_1, \mathbf{v}_2, \Omega_1, \Omega_2$  and  $\{\beta_b, \Omega_b\}_{b \in \mathcal{B}}$ , where  $L$  is the length of the position vector  $\mathbf{p}_1$ . We stack the unknown parameters into a vector and denote it as  $\mathbf{x} = [\mathbf{p}_1^T, \mathbf{p}_2^T, \mathbf{v}_1^T, \mathbf{v}_2^T, \Omega_1, \Omega_2, \{\beta_b, \Omega_b\}_{b \in \mathcal{B}}]^T$ . Let  $\hat{\mathbf{x}}$  be an estimate of  $\mathbf{x}$ . To simplify the computations, we use the modified Bayesian CRLB [23]–[25], which allows us to first treat the sensor clock skews  $\beta_1$  and  $\beta_2$  as known values, and then taking expectation over all

random clock skews. The actual Bayesian CRLB gives a tighter error bound, but has a much more complicated form that unfortunately does not provide additional insights compared to the analysis in this paper. We therefore choose to present the modified Bayesian CRLB instead. We have

$$\mathbb{E} \{ (\hat{\mathbf{x}} - \mathbf{x})(\hat{\mathbf{x}} - \mathbf{x})^T \} \geq \mathbf{F}_{\mathbf{x}}^{-1},$$

where  $\mathbf{F}_{\mathbf{x}}$  is the Fisher information matrix (FIM), which can be shown to be<sup>1</sup>

$$\mathbf{F}_{\mathbf{x}} = \mathbb{E}_{\beta} \left\{ \mathbb{E}_{\mathbf{r}, \mathbf{v} | \mathbf{x}} \left\{ - \frac{\partial^2 \ln p(\mathbf{r}, \mathbf{v} | \mathbf{x}, \beta_1, \beta_2)}{\partial \mathbf{x} \partial \mathbf{x}^T} \right\} \right\}, \quad (8)$$

where  $\beta = \{\beta_m\}_{m \in S \cup B}$  are the random clock skews [24], [25].

#### A. Derivation of $\mathbf{F}_{\mathbf{x}}$

We first map the parameter vector  $\mathbf{x}$  into another parameter vector  $\mathbf{y} = [y_0, y_1, \dots, y_N]^T$ , where  $y_0 = [\mathcal{T}_{1,2}, \mathcal{D}_{1,2}, \Omega_1, \Omega_2]$  and  $y_b = [\mathcal{T}_{1,b}, \mathcal{T}_{2,b}, \mathcal{D}_{1,b}, \mathcal{D}_{2,b}, \beta_b, \Omega_b]$  for  $b \in \mathcal{B}$ . The FIM for  $\mathbf{x}$  can then be shown to be

$$\frac{P_0}{2} \mathbf{F}_{\mathbf{x}} = \mathbb{E}_{\beta} \{ \mathbf{J} \mathbf{F}_{\mathbf{y}} \mathbf{J}^T \}, \quad (9)$$

where  $\mathbf{F}_{\mathbf{y}}$  is the FIM for  $\mathbf{y}$ , and  $\mathbf{J}$  is the Jacobian matrix for the transformation from  $\mathbf{x}$  to  $\mathbf{y}$ , i.e.,  $\mathbf{J} = \partial \mathbf{y} / \partial \mathbf{x}$ . To derive the expression for  $\mathbf{J}$ , we first obtain  $\partial \mathcal{T}_{1,2} / \partial \mathbf{p}_1 = \mathbf{u}_{1,2} / c$ ,  $\partial \mathcal{D}_{1,2} / \partial \mathbf{v}_1 = -f_0 \mathbf{u}_{1,2} / c$ , and

$$\frac{\partial \mathcal{D}_{1,2}}{\partial \mathbf{p}_1} = -\frac{1}{c} \underbrace{\frac{\mathbf{I} - \mathbf{u}_{1,2} \mathbf{u}_{1,2}^T}{\|\mathbf{p}_1 - \mathbf{p}_2\|} (\mathbf{v}_1 - \mathbf{v}_2)}_{\triangleq \mathbf{w}_{1,2}} f_0,$$

where  $\mathbf{w}_{1,2}$  is the orthogonal projection of  $f_0(\mathbf{v}_1 - \mathbf{v}_2)$  onto a direction normal to  $\mathbf{u}_{1,2}$ . Similarly, we have  $\partial \mathcal{D}_{j,b} / \partial \mathbf{v}_j = -f_b \mathbf{u}_{j,b} / c$  and

$$\frac{\partial \mathcal{D}_{j,b}}{\partial \mathbf{p}_j} = -\frac{1}{c} \cdot \underbrace{\frac{\mathbf{I} - \mathbf{u}_{j,b} \mathbf{u}_{j,b}^T}{\|\mathbf{p}_j - \mathbf{p}_b\|} \mathbf{v}_j}_{\triangleq \mathbf{w}_{j,b}} f_b, \quad (10)$$

<sup>1</sup>The notation  $\mathbb{E}_{p(y|x)}$  means taking the expectation over  $y$  conditioned on  $x$ , while  $p(y|x)$  is the probability density function of  $y$  conditioned on  $x$ .

where  $\mathbf{w}_{j,b}$  is orthogonal to  $\mathbf{u}_{j,b}$ . Utilizing these facts, it can be shown that  $\mathbf{J} \in \mathbb{R}^{(4L+2+2N) \times (4+6N)}$  and  $\mathbf{J} = \partial \mathbf{y} / \partial \mathbf{x} = [\mathbf{J}_0^T, \mathbf{J}_1^T, \dots, \mathbf{J}_b^T, \dots, \mathbf{J}_N^T]$ , where

$$\mathbf{J}_0 = \left( \frac{\partial \mathbf{y}_0}{\partial \mathbf{x}} \right)^T = \left[ \begin{array}{c|cc} \mathbf{L}_0 & \mathbf{0} & \\ \hline \mathbf{0} & \mathbf{I}_2 & \mathbf{0} \end{array} \right],$$

and

$$\mathbf{J}_b = \left( \frac{\partial \mathbf{y}_b}{\partial \mathbf{x}} \right)^T = \left[ \begin{array}{c|cc} \mathbf{L}_b & \mathbf{0} & \\ \hline \mathbf{0} & \mathbf{0}_{2 \times 2(b+1)} & \mathbf{I}_2 \quad \mathbf{0} \end{array} \right],$$

with

$$\mathbf{L}_0 = \begin{bmatrix} \frac{1}{c} \mathbf{u}_{1,2}^T & -\frac{1}{c} \mathbf{u}_{1,2}^T & \mathbf{0} & \mathbf{0} \\ -\frac{1}{c} \mathbf{w}_{1,2}^T & \frac{1}{c} \mathbf{w}_{1,2}^T & -\frac{f_0}{c} \mathbf{u}_{1,2}^T & \frac{f_0}{c} \mathbf{u}_{1,2}^T \end{bmatrix}, \quad (11)$$

and

$$\mathbf{L}_b = \begin{bmatrix} \frac{1}{c} \mathbf{u}_{1,b}^T & \mathbf{0} & \mathbf{0} & \mathbf{0} \\ \mathbf{0} & \frac{1}{c} \mathbf{u}_{2,b}^T & \mathbf{0} & \mathbf{0} \\ -\frac{1}{c} \mathbf{w}_{1,b}^T & \mathbf{0} & -\frac{f_b}{c} \mathbf{u}_{1,b}^T & \mathbf{0} \\ \mathbf{0} & -\frac{1}{c} \mathbf{w}_{2,b}^T & \mathbf{0} & -\frac{f_b}{c} \mathbf{u}_{2,b}^T \end{bmatrix}, \quad (12)$$

where  $\mathbf{I}_2$  is a  $2 \times 2$  identity matrix,  $\mathbf{0}_{a \times b}$  is a  $a \times b$  zero matrix, and the notation  $\mathbf{0}$  represents a zero matrix of the appropriate dimensions, which are easily inferred from the context.

Utilizing the well known expression for the complex Gaussian CRLB [26, p.525], the matrix  $\mathbf{F}_y$  can be obtained as from (8) and (9) as

$$\mathbf{F}_y = \sum_b \mathcal{R}e \left\{ \sum_l \frac{\partial \mu_b^*[l]}{\partial \mathbf{y}} \left( \frac{\partial \mu_b[l]}{\partial \mathbf{y}} \right)^T \right\} + \sum_b \mathcal{R}e \left\{ \sum_l \frac{\partial \theta_b^*[l]}{\partial \mathbf{y}} \left( \frac{\partial \theta_b[l]}{\partial \mathbf{y}} \right)^T \right\}. \quad (13)$$

Notice that  $\partial \mu_b[l] / \partial \mathbf{y}_a = 0$  and  $\partial \theta_b[l] / \partial \mathbf{y}_a = 0$  for all  $a \neq b$ , so that  $\mathbf{F}_y$  is a block matrix with structure

$$\mathbf{F}_y = \left[ \begin{array}{c|ccc} \sum_{b \in \mathcal{B}} \mathbf{H}_b & \mathbf{K}_1 & \cdots & \mathbf{K}_N \\ \hline \mathbf{K}_1^T & \mathbf{E}_1 & \cdots & \mathbf{0} \\ \vdots & \vdots & \ddots & \vdots \\ \mathbf{K}_N^T & \mathbf{0} & \cdots & \mathbf{E}_N \end{array} \right],$$

where

$$\begin{aligned}\mathbf{E}_b &= \mathcal{R}e \left\{ \sum_l \frac{\partial \mu_b^*[l]}{\partial \mathbf{y}_b} \left( \frac{\partial \mu_b[l]}{\partial \mathbf{y}_b} \right)^T \right\} + \mathcal{R}e \left\{ \sum_l \frac{\partial \theta_b^*[l]}{\partial \mathbf{y}_b} \left( \frac{\partial \theta_b[l]}{\partial \mathbf{y}_b} \right)^T \right\}, \\ \mathbf{H}_b &= \mathcal{R}e \left\{ \sum_l \frac{\partial \mu_b^*[l]}{\partial \mathbf{y}_0} \left( \frac{\partial \mu_b[l]}{\partial \mathbf{y}_0} \right)^T \right\} + \mathcal{R}e \left\{ \sum_l \frac{\partial \theta_b^*[l]}{\partial \mathbf{y}_0} \left( \frac{\partial \theta_b[l]}{\partial \mathbf{y}_0} \right)^T \right\}, \\ \mathbf{K}_b &= \mathcal{R}e \left\{ \sum_l \frac{\partial \mu_b^*[l]}{\partial \mathbf{y}_0} \left( \frac{\partial \mu_b[l]}{\partial \mathbf{y}_b} \right)^T \right\} + \mathcal{R}e \left\{ \sum_l \frac{\partial \theta_b^*[l]}{\partial \mathbf{y}_0} \left( \frac{\partial \theta_b[l]}{\partial \mathbf{y}_b} \right)^T \right\},\end{aligned}$$

for  $b = 1, \dots, N$ . Substituting  $\mathbf{J}$  and  $\mathbf{F}_y$  into (9), we have

$$\frac{P_0}{2} \mathbf{F}_x = \sum_{b \in \mathcal{B}} \mathbb{E}_\beta \{ \mathbf{J}_0^T \mathbf{H}_b \mathbf{J}_0 + \mathbf{J}_b^T \mathbf{E}_b \mathbf{J}_b + \mathbf{J}_b^T \mathbf{K}_b^T \mathbf{J}_0 + \mathbf{J}_0^T \mathbf{K}_b \mathbf{J}_b \}. \quad (14)$$

### B. Equivalent Fisher Information Matrix

To gain further insights into the structure of  $\mathbf{F}_x$ , we partition the matrices  $\mathbf{E}_b$  such that

$$\mathbf{E}_b = \begin{bmatrix} \mathbf{A}_{E,b} & \mathbf{B}_{E,b} \\ \mathbf{B}_{E,b}^T & \mathbf{D}_{E,b} \end{bmatrix},$$

where  $\mathbf{A}_{E,b} \in \mathbb{R}^{4 \times 4}$ ,  $\mathbf{B}_{E,b} \in \mathbb{R}^{4 \times 2}$ , and  $\mathbf{D}_{E,b} \in \mathbb{R}^{2 \times 2}$ . Similarly, we have

$$\mathbf{H}_b = \begin{bmatrix} \mathbf{A}_{H,b} & \mathbf{B}_{H,b} \\ \mathbf{B}_{H,b}^T & \mathbf{D}_{H,b} \end{bmatrix},$$

where  $\mathbf{A}_{H,b}, \mathbf{B}_{H,b}, \mathbf{D}_{H,b} \in \mathbb{R}^{2 \times 2}$  and

$$\mathbf{K}_b = \begin{bmatrix} \mathbf{A}_{K,b} & \mathbf{B}_{K,b} \\ \mathbf{C}_{K,b} & \mathbf{D}_{K,b} \end{bmatrix},$$

where  $\mathbf{A}_{K,b} \in \mathbb{R}^{2 \times 4}$ ,  $\mathbf{B}_{K,b} \in \mathbb{R}^{2 \times 2}$ ,  $\mathbf{C}_{K,b} \in \mathbb{R}^{2 \times 4}$ , and  $\mathbf{D}_{K,b} \in \mathbb{R}^{2 \times 2}$ . Substituting these matrices into

(14), we obtain after some algebra,

$$\frac{P_0}{2} \mathbf{F}_x = \mathbb{E}_\beta$$

$$\begin{bmatrix} \sum_{b \in \mathcal{B}} \Sigma_b & \sum_{b \in \mathcal{B}} (\mathbf{L}_0^T \mathbf{B}_{H,b} + \mathbf{L}_b^T \mathbf{C}_{K,b}) & \mathbf{L}_0^T \mathbf{B}_{K,1} + \mathbf{L}_1^T \mathbf{B}_{E,1} & \cdots & \mathbf{L}_0^T \mathbf{B}_{K,N} + \mathbf{L}_N^T \mathbf{B}_{E,N} \\ \sum_{b \in \mathcal{B}} (\mathbf{B}_{H,b}^T \mathbf{L}_0 + \mathbf{C}_{K,b} \mathbf{L}_b) & \sum_{b \in \mathcal{B}} \mathbf{D}_{H,b} & \mathbf{D}_{K,1} & \cdots & \mathbf{D}_{K,N} \\ \mathbf{B}_{K,1}^T \mathbf{L}_0 + \mathbf{B}_{E,1}^T \mathbf{L}_1 & \mathbf{D}_{K,1}^T & \mathbf{D}_{E,1} & \cdots & \mathbf{0} \\ \vdots & \vdots & \vdots & \ddots & \vdots \\ \mathbf{B}_{K,N}^T \mathbf{L}_0 + \mathbf{B}_{E,N}^T \mathbf{L}_N & \mathbf{D}_{K,N}^T & \mathbf{0} & \cdots & \mathbf{D}_{E,N} \end{bmatrix}, \quad (15)$$

with  $\Sigma_b = \mathbf{L}_b^T \mathbf{A}_{E,b} \mathbf{L}_b + \mathbf{L}_0^T \mathbf{A}_{H,b} \mathbf{L}_0 + \mathbf{L}_0^T \mathbf{A}_{K,b} \mathbf{L}_b + \mathbf{L}_b^T \mathbf{A}_{K,b}^T \mathbf{L}_0$ . Since we are interested in estimation accuracies for sensor locations and velocities, i.e.,  $\{\mathbf{p}_j, \mathbf{v}_j\}_{j=1,2}$ , it is sufficient to find its equivalent Fisher information matrix (EFIM)  $\mathbf{F}_{e,s}$  [18], [23], which is given by

$$\frac{P_0}{2} \mathbf{F}_{e,s} = \sum_{b \in \mathcal{B}} \mathbb{E}_{\beta} \{ \Sigma_b \} - \mathbb{E}_{\beta} \{ \mathbf{F}_1 \} \mathbb{E}_{\beta} \{ \mathbf{F}_2 \}^{-1} \mathbb{E}_{\beta} \{ \mathbf{F}_1 \}^T,$$

where  $\mathbf{F}_1$  and  $\mathbf{F}_2$  represent the upper- and lower-right-corner block of  $\mathbf{F}_x$  in (15), respectively.

Therefore, it follows that

$$\frac{P_0}{2} \mathbf{F}_{e,s} = \sum_{b \in \mathcal{B}} \mathbf{Q}_b - \left( \sum_{b \in \mathcal{B}} \mathbf{U}_b \right) \left( \sum_{b \in \mathcal{B}} \mathbf{V}_b \right)^{-1} \left( \sum_{b \in \mathcal{B}} \mathbf{U}_b^T \right), \quad (16)$$

where

$$\begin{aligned} \mathbf{Q}_b &= \mathbf{L}_b^T (\bar{\mathbf{A}}_{E,b} - \bar{\mathbf{B}}_{E,b} \bar{\mathbf{D}}_{E,b}^{-1} \bar{\mathbf{B}}_{E,b}^T) \mathbf{L}_b + \mathbf{L}_0^T (\bar{\mathbf{A}}_{H,b} - \bar{\mathbf{B}}_{K,b} \bar{\mathbf{D}}_{E,b}^{-1} \bar{\mathbf{B}}_{K,b}^T) \mathbf{L}_0 \\ &\quad + \mathbf{L}_0^T (\bar{\mathbf{A}}_{K,b} - \bar{\mathbf{B}}_{K,b} \bar{\mathbf{D}}_{E,b}^{-1} \bar{\mathbf{B}}_{E,b}^T) \mathbf{L}_b + \mathbf{L}_b^T (\bar{\mathbf{A}}_{K,b}^T - \bar{\mathbf{B}}_{E,b} \bar{\mathbf{D}}_{E,b}^{-1} \bar{\mathbf{B}}_{K,b}^T) \mathbf{L}_0, \\ \mathbf{U}_b &= \mathbf{L}_0^T (\bar{\mathbf{B}}_{H,b} - \bar{\mathbf{B}}_{K,b} \bar{\mathbf{D}}_{E,b}^{-1} \bar{\mathbf{D}}_{K,b}^T) + \mathbf{L}_b^T (\bar{\mathbf{C}}_{K,b}^T - \bar{\mathbf{B}}_{E,b} \bar{\mathbf{D}}_{E,b}^{-1} \bar{\mathbf{D}}_{K,b}^T), \\ \mathbf{V}_b &= \bar{\mathbf{D}}_{H,b} - \bar{\mathbf{D}}_{K,b} \bar{\mathbf{D}}_{E,b}^{-1} \bar{\mathbf{D}}_{K,b}^T, \end{aligned}$$

with  $\bar{\mathbf{A}} = \mathbb{E}_{\beta} \{ \mathbf{A} \}$  for any matrix  $\mathbf{A}$ .

To facilitate further analysis of the EFIM in (16), we define the signal energy  $P_b$ , the root-mean-square (RMS) bandwidth  $W_b$ , and the RMS integration time  $T_b$  for the signal  $g_b(t)$  as [27],

$$P_b = \int |g_b(t)|^2 dt, \quad W_b = \left[ \frac{\int |f G_b(f)|^2 df}{\int |G_b(f)|^2 df} \right]^{\frac{1}{2}}, \quad T_b = \left[ \frac{\int |t g_b(t)|^2 dt}{\int |g_b(t)|^2 dt} \right]^{\frac{1}{2}}.$$

Without loss of generality, we assume that the signal  $g_b(t)$  has zero centroid in time and frequency, hence  $W_b$  and  $T_b$  characterize the signal's energy dispersion around its centroid in time and frequency, respectively. In the following, we make various assumptions and approximations, which hold in most practical applications. We use  $a \ll b$  to mean that  $a/b$  can be approximated by 0.

### Assumption 1

(i) The clock skew standard deviations  $\sigma_{\beta_m} < 1$  for all  $m \in \mathcal{S} \cup \mathcal{B}$ .

(ii) For every beacon  $b \in \mathcal{B}$ , the RMS bandwidth  $W_b$  is much smaller than the nominal carrier frequency  $f_b$  with  $W_b \ll f_b$ .

(iii) There exists  $\epsilon > 0$  and a measurable set with probability at least  $1 - \epsilon$  so that  $\mathcal{T}_{1,2} \ll \mathbb{T}_b/3$ ,  $\mathcal{T}_{j,b} \ll \mathbb{T}_b/3$ , and  $\Omega_j \ll \beta_j \mathbb{T}_b/3$ , for  $j = 1, 2$  and for every beacon  $b \in \mathcal{B}$ . Furthermore,  $\epsilon$  can be chosen sufficiently small so that all expectations can be approximated by taking expectations over this set.

For each  $b \in \mathcal{B}$ , let  $\text{SNR}_b = P_b/P_0$  be the effective output signal-to-noise ratio of the received signal from  $b$ . As shown in [28], the effective output  $\text{SNR}_b$  depends on the input SNR and the bandwidth-time product  $W_b \mathbb{T}_b$ . Let

$$\lambda_b = \frac{8\pi^2 W_b^2 \text{SNR}_b}{c^2}, \text{ and } \epsilon_b = \frac{8\pi^2 \mathbb{T}_b^2 \text{SNR}_b}{c^2}. \quad (17)$$

We have the following theorem, whose proof is given in Appendix C.

**Theorem 2** *Suppose that Assumption 1 holds. Let  $\phi_b = [\mathbf{u}_{1,b}^T, -\mathbf{u}_{2,b}^T]^T$ ,  $\phi_s = [\mathbf{u}_{1,2}^T, -\mathbf{u}_{1,2}^T]^T$ ,  $\rho_b = [\mathbf{w}_{1,b}^T, -\mathbf{w}_{2,b}^T]^T$ , and  $\rho_s = [\mathbf{w}_{1,2}^T, -\mathbf{w}_{1,2}^T]^T$ . Treating the sensor clock skews as nuisance parameters, the EFIM for estimating the sensors' locations and velocities at sensor  $S_1$ , denoted as  $\mathbf{F}_{e,s}$ , is approximately given by*

$$\mathbf{F}_{e,s} = \frac{1}{2} \sum_b \begin{bmatrix} \lambda_b(\Phi_b - \Xi) + \epsilon_b(1 - \sigma_{\beta_b}^2)^{-1} \mathbf{P}_b & \epsilon_b(1 - \sigma_{\beta_b}^2)^{-1} \mathbf{\Gamma}_b \\ \epsilon_b(1 - \sigma_{\beta_b}^2)^{-1} \mathbf{\Gamma}_b^T & \epsilon_b(1 - \sigma_{\beta_b}^2)^{-1} \mathbf{\Pi}_b \end{bmatrix}, \quad (18)$$

where we let  $\bar{\lambda}_b = \frac{\lambda_b}{\sum_{b'} \lambda_{b'}}$ ,  $\sigma_s = 2[1 + (\sigma_{\beta_1}^2 - 3\sigma_{\beta_1}^2 \sigma_{\beta_2}^2)/(1 - 3\sigma_{\beta_2}^2 + \sigma_{\beta_1}^2 \sigma_{\beta_2}^2)]$ , and

$$\Xi = \sigma_s \sum_b \bar{\lambda}_b (\phi_b - \phi_s) \sum_b \bar{\lambda}_b (\phi_b - \phi_s)^T,$$

$$\Phi_b = (\phi_b - \phi_s)(\phi_b - \phi_s)^T,$$

$$\mathbf{P}_b = (\rho_b - \rho_s)(\rho_b - \rho_s)^T,$$

$$\mathbf{\Pi}_b = (f_b \phi_b - f_0 \phi_s)(f_b \phi_b - f_0 \phi_s)^T,$$

$$\mathbf{\Gamma}_b = (\rho_b - \rho_s)(f_b \phi_b - f_0 \phi_s)^T.$$

Theorem 2 provides an approximate lower bound for the location and velocity estimation errors. However, since we have used the modified Bayesian CRLB, this bound is not tight. Nevertheless, the information bound in Theorem 2 gives us various insights into the problem of location and velocity estimation, which we discuss below.

1) We see from (18) that the EFIM consists of various “information matrix” components, which we describe in the following.

- The matrix  $\Phi_b$  can be interpreted as the ranging direction matrix (RDM) associated with the directions  $\mathbf{u}_{1,b} - \mathbf{u}_{1,2}$  and  $\mathbf{u}_{2,b} - \mathbf{u}_{1,2}$ . This is similar to the RDM introduced in [18], where the EFIM is derived in the case where a single sensor localizes with the aid of synchronized anchors so that  $\mathbf{u}_{1,2} = \mathbf{0}$ . Similar to [18], we can interpret  $\lambda_b$  as the *ranging information intensity*, which is a constant that depends only on beacon characteristics like SNR. We note that the beacon clock skews do not affect the ranging information intensity or the RDM, which is intuitively correct as TDOA ranging is not affected by beacon clock skews.
- Let  $\mathbf{u}^\perp$  be the unit vector orthogonal to  $\mathbf{u}$ . The vectors  $\rho_b$  and  $\rho_s$  contain Doppler shift information in the directions  $\mathbf{u}_{1,b}^\perp$  and  $\mathbf{u}_{1,2}^\perp$  respectively. Therefore, the matrix  $\mathbf{P}_b$  can be interpreted as the relative Doppler information matrix associated with the directions  $\mathbf{u}_{1,b}^\perp$ ,  $\mathbf{u}_{2,b}^\perp$  and  $\mathbf{u}_{1,2}^\perp$ . This is intuitively appealing as all location information in the directions  $\mathbf{u}_{1,b}$ ,  $\mathbf{u}_{2,b}$ , and  $\mathbf{u}_{1,2}$  have already been captured in  $\Phi_b$  so that  $\mathbf{P}_b$  contains additional information in directions orthogonal to these. Moreover, since Doppler shift is affected by beacon clock skews, we have a factor of  $(1 - \sigma_{\beta_b}^2)^{-1}$  multiplied to  $\mathbf{P}_b$  in (18). We can also interpret  $\epsilon_b$  as the *Doppler information intensity*.
- The term  $f_b \phi_b$  is the rate of change of Doppler shift in the direction  $\mathbf{u}_{j,b}$  w.r.t.  $\mathbf{v}_j$ . Therefore, the matrix  $\mathbf{\Pi}_b$  contains information associated with how fast the Doppler shift along the directions  $\mathbf{u}_{j,b}$  is changing w.r.t. that along  $\mathbf{u}_{1,2}$ . This is mainly useful for velocity estimation, and so do not appear in the CRLB derived in [9], [18]. Beacon clock skews affect the information contained in  $\mathbf{\Pi}_b$  and appears in the multiplicative factor  $(1 - \sigma_{\beta_b}^2)^{-1}$  in (18).
- The term  $\Xi$  contains the weighted average ranging information from all beacons, with the weight of beacon  $b$  being  $\lambda_b$  normalized by the sum of all ranging information intensities. Since  $S_2$  transmits all its received signals from the beacons to  $S_1$ , we can interpret  $\Xi$  as the collective effect of sensor clock asynchronism on the information transmitted from  $S_2$ .

2) From (18), it is clear that the EFIM for sensor locations and velocities depend on neither the value of beacon clock offsets nor the value of sensor clocks offsets. This suggests that there

exists estimation algorithms that can eliminate *both* beacon and sensor clock offsets. It can be shown that the TDOA procedure cancels out the beacon clock offsets. We will show in Section IV-B that the DTDOA method allows us to cancel out sensor clock offsets as well.

- 3) Although the size of clock offsets do not affect the EFIM, we observe that there is loss of information whenever sensor clocks are not synchronized. Consider the case where the two sensors are static, so that  $\boldsymbol{\rho}_b = \mathbf{0}$  and  $\boldsymbol{\rho}_s = \mathbf{0}$ . The EFIM in (18) for sensor locations reduces to

$$\mathbf{F}_{e,static} = \frac{1}{2} \sum_b \lambda_b (\boldsymbol{\Phi}_b - \boldsymbol{\Xi}). \quad (19)$$

On the other hand, if sensors and beacons are static and synchronized, it can be shown that the EFIM is given by

$$\mathbf{F}_{e,syn} = \sum_b \lambda_b \left( \boldsymbol{\Phi}_b + \begin{bmatrix} \mathbf{u}_{1,b} \mathbf{u}_{1,2}^T + \mathbf{u}_{1,2} \mathbf{u}_{1,b}^T & \mathbf{u}_{1,b} (\mathbf{u}_{2,b} - \mathbf{u}_{1,2})^T \\ (\mathbf{u}_{2,b} - \mathbf{u}_{1,2}) \mathbf{u}_{1,b}^T & \mathbf{0} \end{bmatrix} \right). \quad (20)$$

Therefore, the information loss due to sensor clock offsets is given by  $\mathbf{F}_{e,syn} - \mathbf{F}_{e,static}$  which is non-zero. It can be seen that the information loss does not depend on the value of sensor clock offsets, suggesting that clock offsets can be eliminated but at the price of a constant information loss.

- 4) As can be seen from (18), the EFIM depends on direction vectors  $\mathbf{u}_{j,b}$  and  $\mathbf{u}_{1,2}$  which are determined only by the relative positions of sensors and beacons. To analyze the effect of beacon-sensor geometry on the localization performance, we consider the case (19) in two dimensional space with static sensors and beacons uniformly distributed on a circle centered at  $S_1$ . Letting the angle from beacon  $b$  to  $S_j$  be  $\kappa_{j,b}$ , we obtain  $\mathbf{u}_{j,b} = [\cos \kappa_{j,b}, \sin \kappa_{j,b}]^T$ . As the radius of the circle increases, we have in the limit of infinite radius,  $\kappa_{1,b} = \kappa_{2,b}$  so that

$$\lim_{\|\mathbf{p}_b - \mathbf{p}_1\| \rightarrow \infty} \mathbf{u}_{1,b} = \lim_{\|\mathbf{p}_b - \mathbf{p}_2\| \rightarrow \infty} \mathbf{u}_{2,b} \triangleq \check{\mathbf{u}}_b.$$

The EFIM in (19) then reduces to

$$\mathbf{F}_{e,static} = \sum_b \frac{\lambda_b}{2} \begin{bmatrix} \check{\boldsymbol{\Phi}}_b & -\check{\boldsymbol{\Phi}}_b \\ -\check{\boldsymbol{\Phi}}_b & \check{\boldsymbol{\Phi}}_b \end{bmatrix},$$

with  $\check{\Phi}_b = (\check{\mathbf{u}}_b + \check{\mathbf{u}}_{1,2})(\check{\mathbf{u}}_b + \check{\mathbf{u}}_{1,2})^T - \sigma_s \sum_b \bar{\lambda}_b \check{\mathbf{u}}_b \sum_b \bar{\lambda}_b \check{\mathbf{u}}_b^T - \sigma_s \sum_b \bar{\lambda}_b \check{\mathbf{u}}_b \mathbf{u}_{1,2}^T - \sigma_s \mathbf{u}_{1,2} \sum_b \bar{\lambda}_b \check{\mathbf{u}}_b^T - \sigma_s \mathbf{u}_{1,2} \mathbf{u}_{1,2}^T$ . It is clear that the corresponding EFIM  $\mathbf{F}_{e,s}$  is rank-deficient, which implies that large estimation errors will be introduced when beacons are too far away from the sensors.

5) Suppose that sensor  $S_2$  has known location and velocity. We then have a simpler expression for the EFIM. We have  $\phi_b = \mathbf{u}_{1,b}$ ,  $\phi_s = \mathbf{u}_{1,2}$ ,  $\rho_b = \mathbf{w}_{1,b}$  and  $\rho_s = \mathbf{w}_{1,2}$ , with  $\Phi_b = (\mathbf{u}_{1,b} - \mathbf{u}_{1,2})(\mathbf{u}_{1,b} - \mathbf{u}_{1,2})^T$ ,  $\mathbf{P}_b = (\mathbf{w}_{1,b} - \mathbf{w}_{1,2})(\mathbf{w}_{1,b} - \mathbf{w}_{1,2})^T$ ,  $\mathbf{\Pi}_b = (f_b \mathbf{u}_{1,b} - f_0 \mathbf{u}_{1,2})(f_b \mathbf{u}_{1,b} - f_0 \mathbf{u}_{1,2})^T$ , and  $\mathbf{\Gamma}_b = (\mathbf{w}_{1,b} - \mathbf{w}_{1,2})(f_b \mathbf{u}_{1,b} - f_0 \mathbf{u}_{1,2})^T$ . In this case,  $S_2$  acts almost like an anchor, except that it does not transmit its own independent signal. Therefore the amount of information available to  $S_1$  is less than that of a true anchor.

#### IV. LOCATION AND VELOCITY ESTIMATION OF TWO SENSORS

In this section, we consider the use of TDOA and FDOA for location and velocity estimation when sensor and beacon clocks are not synchronized. We first evaluate the effect of clock asynchronism on TDOA and FDOA estimates, and then propose a DTDOA method to mitigate its effects.

##### A. TDOA and FDOA Estimation

The TDOA and FDOA measurements between two sensors are obtained by maximizing the amplitude of the complex ambiguity function  $\mathcal{A}(\tau, \xi)$ . At the sensor  $S_1$ , the ambiguity function w.r.t. beacon  $b$  can be obtained as

$$\mathcal{A}(\tau, \xi) \propto \int V_{1,b}(\beta_1 f) R_{1,b}^*[\beta_1(f - \xi)] e^{i2\pi 2\pi f \tau} df. \quad (21)$$

Substituting (4) and (5) into (21), and maximizing  $|\mathcal{A}(\tau, \xi)|$  w.r.t  $\tau$  and  $\xi$ , the optimal solution for TDOA and FDOA estimates is then given by

$$\hat{\tau}_b \approx \beta_1 \mathcal{T}_{2,b} - \beta_1 \mathcal{T}_{1,b} + \beta_1 \mathcal{T}_{1,2} + \Omega_1 - \frac{\beta_1}{\beta_2} \Omega_2 + e_b^\tau, \quad (22)$$

$$\hat{\xi}_b \approx \frac{\beta_b}{\beta_1} \mathcal{D}_{2,b} - \frac{\beta_b}{\beta_1} \mathcal{D}_{1,b} + \left[ \frac{\beta_2}{\beta_1} + \frac{f_b}{f_0} \left( \frac{\beta_b}{\beta_1} - \frac{\beta_2}{\beta_1} \right) \right] \mathcal{D}_{1,2} + \left( 1 - \frac{\beta_2}{\beta_1} \right) (f_b - f_0) + e_b^\xi, \quad (23)$$

for  $b \in \mathcal{B}$ , where  $e_n^\tau$  and  $e_n^f$  denotes estimation errors for TDOA and FDOA respectively, and we have approximated  $\gamma_{2,b} \approx 1$  and  $\gamma_{1,2} \approx 1$  since  $\|\mathbf{v}_1\| \ll c$  and  $\|\mathbf{v}_2\| \ll c$ . It can be seen that both the TDOA estimate  $\hat{\tau}_b$  and the FDOA estimate  $\hat{\xi}_b$  include a bias term, which are due to asynchronous clocks and communication distortion between two sensors  $S_2$  and  $S_1$ .

## B. Location and Velocity Estimation

Suppose there exist  $N$  beacons around  $S_2$  and  $S_1$ , a set of TDOA and FDOA estimates,  $\{\hat{\tau}_b, \hat{\xi}_b\}_{b \in \mathcal{B}}$ , can be obtained at each sensor. We in the following propose an algorithm to estimate sensor locations and velocities using TDOA and FDOA measurements.

1) *Location Estimation*: Let  $\beta_j = 1 + \delta_{\beta_j}$  with  $\delta_{\beta_j}$  being a random error such that  $\mathbb{E}\{\delta_{\beta_j}\} = 0$  and  $\mathbb{E}\{\delta_{\beta_j}^2\} = \sigma_{\beta_j}^2$ . Substituting into (22), we have

$$c\hat{\tau}_b = \|\mathbf{p}_2 - \mathbf{p}_b\| - \|\mathbf{p}_1 - \mathbf{p}_b\| + c(\mathcal{T}_{1,2} + \Omega_1 - \Omega_2) + c(\delta_b^\tau + e_b^\tau), \quad (24)$$

where  $\delta_b^\tau = \delta_{\beta_1}(\|\mathbf{p}_2 - \mathbf{p}_b\| - \|\mathbf{p}_1 - \mathbf{p}_b\| + \|\mathbf{p}_1 - \mathbf{p}_2\|) - c\Omega_2(1 + \delta_{\beta_1})/(1 + \delta_{\beta_2})$ . It can be seen that the noise term  $\delta_b^\tau$  depends on the parameters due to  $\delta_{\beta_1}$ . However, if  $\sigma_{\beta_j}$  is small, its effect on the location estimation is negligible, and we approximate  $\delta_b^\tau = -c\Omega_2(1 + \delta_{\beta_1})/(1 + \delta_{\beta_2})$ . Since delay estimations from all beacons, i.e.,  $\{\hat{\tau}_b\}_{b \in \mathcal{B}}$ , experience the same amount of biases caused by propagation delay and sensor clock offsets, we subtract two delay estimations and obtain

$$c(\hat{\tau}_b - \hat{\tau}_a) = \underbrace{(\|\mathbf{p}_2 - \mathbf{p}_b\| - \|\mathbf{p}_2 - \mathbf{p}_a\|) - (\|\mathbf{p}_1 - \mathbf{p}_b\| - \|\mathbf{p}_1 - \mathbf{p}_a\|)}_{\triangleq \mathbf{f}_{b,a}(\mathbf{x})} + c(\delta_b^\tau - \delta_a^\tau + e_b^\tau - e_a^\tau), \quad (25)$$

for  $a \neq b$  and  $\mathbf{x} = [\mathbf{p}_1^T, \mathbf{p}_2^T]^T$ . We call the quantity  $c(\hat{\tau}_b - \hat{\tau}_a)$  obtained in (25) the differential TDOA or DTDOA. Suppose there exist  $N$  beacons, multiple DTDOA can be obtained for  $a, b \in \{1, \dots, N\}$ . Stacking all available DTDOA into vectors, we have

$$\mathbf{z} = \mathbf{f}(\mathbf{x}) + \mathbf{e}, \quad (26)$$

where  $\mathbf{f}(\mathbf{x}) = [\dots, \mathbf{f}_{b,a}(\mathbf{x}), \dots]^T$ , similarly  $\mathbf{z} = [\dots, c(\hat{\tau}_b - \hat{\tau}_a), \dots]^T$  and  $\mathbf{e} = [\dots, c(\delta_b^\tau - \delta_a^\tau + e_b^\tau - e_a^\tau), \dots]^T$  with covariance matrix  $\mathbf{Q} = \mathbb{E}\{\mathbf{e}\mathbf{e}^T\}$ . We estimate the sensor locations by minimizing the least square (LS) error criterion,

$$(\hat{\mathbf{p}}_1, \hat{\mathbf{p}}_2) = \arg \min_{\mathbf{x}} (\mathbf{z} - \mathbf{f}(\mathbf{x}))^T \mathbf{Q}^{-1} (\mathbf{z} - \mathbf{f}(\mathbf{x})). \quad (27)$$

A closed-form solution of (27) does not exist in general due to its non-linearity nature. Various algorithms have been investigated in the literature [15], [29]–[35]. Generally, we can linearize  $\mathbf{f}(\mathbf{x})$  by a Taylor series expansion around an initial guess  $\hat{\mathbf{x}}_0$  for the true parameter vector, and we have

$$\mathbf{f}(\mathbf{x}) \approx \mathbf{f}(\hat{\mathbf{x}}_0) + \mathbf{G}(\hat{\mathbf{x}}_0)(\mathbf{x} - \hat{\mathbf{x}}_0), \quad (28)$$

where  $\mathbf{G}(\cdot) = [\cdots, \mathbf{G}_{b,a}^T(\cdot), \cdots]^T$  with  $\mathbf{G}_{b,a}(\hat{\mathbf{x}}_0) \triangleq \nabla_{\mathbf{x}} \mathbf{f}_{b,a}(\mathbf{x})|_{\mathbf{x}=\hat{\mathbf{x}}_0}$  is the gradient of  $\mathbf{f}_{b,a}(\cdot)$  evaluated at  $\mathbf{x} = \hat{\mathbf{x}}_0$  and can be shown as

$$\mathbf{G}_{b,a}(\hat{\mathbf{x}}_0) = \left[ \begin{array}{c} -\frac{\mathbf{p}_1 - \mathbf{p}_b}{\|\mathbf{p}_1 - \mathbf{p}_b\|} + \frac{\mathbf{p}_1 - \mathbf{p}_a}{\|\mathbf{p}_1 - \mathbf{p}_a\|}, \\ \frac{\mathbf{p}_2 - \mathbf{p}_b}{\|\mathbf{p}_2 - \mathbf{p}_b\|} - \frac{\mathbf{p}_2 - \mathbf{p}_a}{\|\mathbf{p}_2 - \mathbf{p}_a\|} \end{array} \right]_{\mathbf{x}=\hat{\mathbf{x}}_0}^T.$$

An iterative solution of (27) by using gradient descent method is then given by

$$\hat{\mathbf{x}}^{(l+1)} = \hat{\mathbf{x}}^{(l)} + \alpha_l (\mathbf{G}^T(\hat{\mathbf{x}}^{(l)}) \mathbf{Q}^{-1} \mathbf{G}(\hat{\mathbf{x}}^{(l)}))^{-1} \mathbf{G}^T(\hat{\mathbf{x}}^{(l)}) \mathbf{Q}^{-1} (\mathbf{z} - \mathbf{f}(\hat{\mathbf{x}}^{(l)})), \quad (29)$$

where  $\alpha_l$  is the step size in the  $l$ -th iteration.

2) *Velocity Estimation:* We utilize FDOA estimates from all beacons, i.e.,  $\{\hat{\xi}_b\}_{b \in \mathcal{B}}$  to estimate the velocities of both sensors. From (23) and  $\beta_m = 1 + \delta_{\beta_m}$  for  $m \in \mathcal{S} \cup \mathcal{B}$ , we have

$$c\hat{\xi}_b = (f_b \hat{\mathbf{u}}_{1,b}^T - f_0 \hat{\mathbf{u}}_{1,2}^T) \mathbf{v}_1 - (f_b \hat{\mathbf{u}}_{2,b}^T - f_0 \hat{\mathbf{u}}_{1,2}^T) \mathbf{v}_2 + c(\delta_b^\xi + e_b^\xi), \quad (30)$$

where  $\hat{\mathbf{u}}_{2,b} = (\hat{\mathbf{p}}_2 - \mathbf{p}_b) / \|\hat{\mathbf{p}}_2 - \mathbf{p}_b\|$ ,  $\hat{\mathbf{u}}_{2,a}$ ,  $\hat{\mathbf{u}}_{1,a}$  and  $\hat{\mathbf{u}}_{1,b}$  are defined similarly, and  $\delta_b^\xi = (\delta_{\beta_b} - \delta_{\beta_1} - \delta_{\beta_b} \delta_{\beta_1}) [(\hat{\mathbf{u}}_{1,b} - \hat{\mathbf{u}}_{1,2})^T \mathbf{v}_1 - (\hat{\mathbf{u}}_{2,b} - \hat{\mathbf{u}}_{1,2})^T \mathbf{v}_2] f_b / c + (\delta_{\beta_2} - \delta_{\beta_1} - \delta_{\beta_2} \delta_{\beta_1}) \hat{\mathbf{u}}_{1,2}^T (\mathbf{v}_1 - \mathbf{v}_2) (f_b - f_0) / c + (\delta_{\beta_1} - \delta_{\beta_2} + \delta_{\beta_1} \delta_{\beta_2}) (f_b - f_0)$ , and we have approximated  $1/(1 + \delta_{\beta_m}) \approx 1 - \delta_{\beta_m}$  for small  $\delta_{\beta_m}$ . The random variable  $\delta_b^\xi$  has zero mean and depends on the velocity and the standard deviation of clock skews. When  $\sigma_{\beta_m}$  is small, its effect is negligible, and we approximate  $\delta_b^\xi = (\delta_{\beta_1} - \delta_{\beta_2} + \delta_{\beta_1} \delta_{\beta_2}) (f_b - f_0)$ . Notice that (30) is linear with respect to the sensor velocities  $\mathbf{v}_1$  and  $\mathbf{v}_2$ , and the noise term has zero mean and known variance, the estimates of sensor velocities can therefore be easily obtained by the BLUE estimator [26].

## V. SIMULATION RESULTS

Simulations are carried out to verify the CRLB and performance of our proposed algorithms. Sensor  $S_2$  starts at location  $[0, 0]$  km and moves with speed 100 km/h (27.8m/s). Sensor  $S_1$  starts at a point 1km away from  $S_2$  and moves at speed 100km/h away from sensor  $S_2$ .  $N$  beacons are uniformly distributed in a circle with a radius 10km, and an example for 8 beacons is shown in Figure 3. The clock skews  $\beta_m$  are drawn from Gamma distributions with  $\mathbb{E}\{\beta_m\} = 1$  and

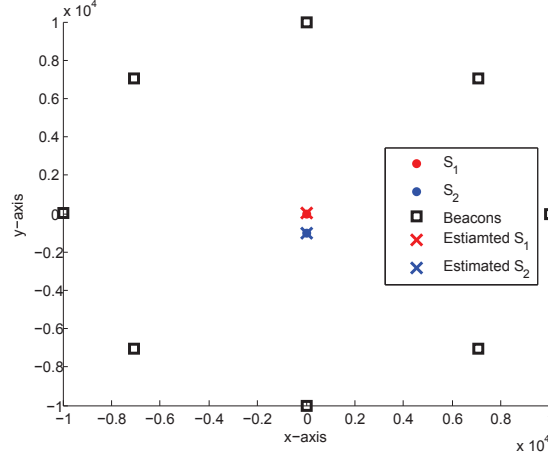


Fig. 3. Positions of beacons and sensors.

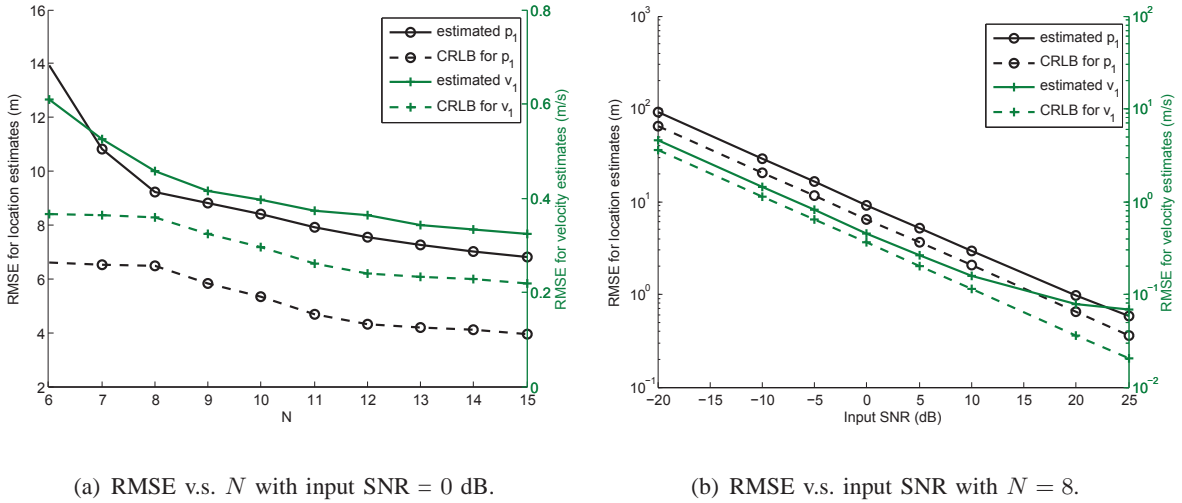


Fig. 4. Effect of measurement noise on CRLB and performance of the proposed algorithm.

varying standard deviations  $\sigma_{\beta_m}$  for  $m \in \mathcal{S} \cup \mathcal{B}$ . The signal bandwidth is set to be 200KHz and the integration time is 1s. For each set of parameters, 10000 simulation runs are performed.

Figure 4 compares the performance of the proposed algorithm with the modified Bayesian CRLB under various number of beacons and measurement noise, where the standard deviations of clock skews are set to  $10^{-6}$ . Since approximations have been made in the algorithm and we used a looser modified CRLB, there exists a performance gap between our algorithm and the bound. When the number of beacons is larger than 8, the RMSE gap for the location and velocity estimates is constant around 3m and 0.1m/s, respectively.

Figure 5 investigates the effect of clock asynchronism on the location and velocity estimation,

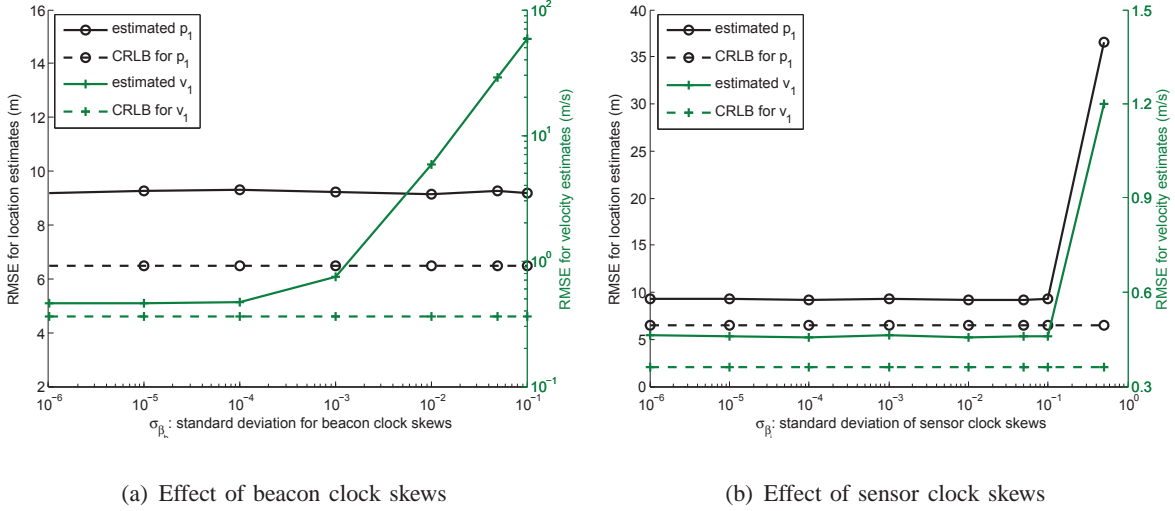


Fig. 5. Effect of clock asynchronism on CRLB and performance of the proposed algorithm.

TABLE II  
RMSE COMPARISON

Estimator	Parameter	$\Omega_1 = 10\text{ms}$	$\Omega_1 = 50\text{ms}$	$\Omega_1 = 100\text{ms}$
DTDOA	$\mathbf{p}_1$ (m)	9.15	9.38	9.58
	$\mathbf{v}_1$ (m/s)	0.45	0.52	0.66
TDOA	$\mathbf{p}_1$ (m)	$0.24 \times 10^7$	$2.18 \times 10^7$	$4.58 \times 10^7$
	$\mathbf{v}_1$ (m/s)	$0.12 \times 10^7$	$1.41 \times 10^8$	$5.09 \times 10^8$

where the number of beacons is set to be 8 and the input SNR is 0 dB. As shown in Figure 5(a) and Figure 5(b), the the modified Bayesian CRLB is hardly affected by the standard deviation of sensor or beacon clock skew. Therefore, the sensor and beacon clock skews have limited impact on the CRLB in most practical applications. The performance of the algorithm deteriorates for larger clock skews, especially for velocity estimation with varying beacon clock skews. This is because we have approximated  $\delta_b^\xi \approx 0$  in (30) which holds only for small  $\delta_{\beta_b}$  and  $\delta_{\beta_j}$ . As the clock skews increase, this approximation will be violated and the estimation error increases. However, we note that when the beacon clock skew is smaller than  $10^{-3}$  and and the sensor clock skew is smaller than  $10^{-1}$ , our proposed algorithm achieves estimation accuracy close to the modified Bayesian CRLB. As the typical value for standard deviations of crystal oscillators ranges from  $10^{-6}$  to  $10^{-3}$ , it can be expected that our algorithm is robust in most situations.

In addition, we compare the performance of our DTDOA estimator with that using TDOA which

does not account for the sensor clock offsets, i.e., the bias term  $\Omega_1 - \Omega_2$  in (24) is not removed. In Table II, we fix  $\Omega_2 = 5\text{ms}$  and increase the value of  $\Omega_1$  from 10ms to 100ms. It can be seen that our estimator is robust to sensor clock offsets and achieves an accuracy smaller than 10m for location estimation, while the accuracy of the estimator using TDOA is at the order of  $10^7\text{m}$  and it deteriorates as the sensor clock offset increases.

## VI. CONCLUSIONS

In this paper, we have considered the problem of localizing two sensors using signals from beacons with known locations. We assume that all beacons and sensors have free-running oscillators that have unknown clock skews and offsets. Each sensor performs self-localization by using TDOA and FDOA measurements between the two sensors. We analyze the biases introduced by asynchronous clocks into the received signals and obtained closed-form expressions for TDOA and FDOA estimates based on these distorted signals. We derive the equivalent Fisher information matrix for the modified Bayesian CRLB using the received signal waveforms. We propose an algorithm for estimating sensor location and velocity based on DTDOA and FDOA estimates. Simulation results show that our algorithm is robust to clock offsets and is close to the modified Bayesian CRLB when clock skews are small.

In this paper, we have assumed for simplicity that sensors forward received signals from the beacons to each other. This may be impractical or may result in high communication costs. Future research includes investigating the more practical scenario where sensor information exchanges are limited in bandwidth and exchange frequency. We have also limited our investigations to static beacons in this paper. The use of mobile beacons like unmanned aerial vehicles and non-GPS satellites is of practical interest.

## APPENDIX A

### PROOF OF PROPOSITION 1

*Proof:* (i) The baseband signal is generated at beacon  $b$ . The frequency scaling and time delay are introduced due to its local oscillator. Since  $\tilde{g}_b(t) = g_b(\beta_b t + \Omega_b)$ , the result follows directly.

(ii) The carrier wave generated at beacon  $b$  is  $\exp\{i2\pi f_b(\beta_b t + \Omega_b)\}$ , and the emitted signal  $\tilde{u}_b(t)$  is obtained by multiplying the baseband signal  $\tilde{g}_b(t)$  with the carrier wave. This operation introduces a frequency and phase shift into the baseband signal, and the result follows easily.

(iii) As discussed in Section II-A, the channel between the  $b$ -th beacon and  $S_j$  can be modeled as  $h_{j,b}(t) = \alpha_{j,b}\delta(\gamma_{j,b}t - \mathcal{T}_{j,b})$ . The received signal  $\tilde{r}_{j,b}(t)$  is obtained by the convolution of the emitted signal  $\tilde{u}_b(t)$  and  $h_{j,b}(t)$ , and we have  $\tilde{r}_{j,b}(t) = \alpha_{j,b}\tilde{u}_b(\gamma_{j,b}t - \mathcal{T}_{j,b})$ , from which the positive frequency part  $\tilde{R}_{j,b}(\xi)$  follows easily.

(iv) The down-conversion of the received signal  $\tilde{r}_{j,b}(t)$  to the baseband is achieved by multiplying  $\tilde{r}_{j,b}(t)$  with a locally generated carrier wave and passing it through a low-pass filter. The carrier wave generated by  $S_j$  is given by  $\exp\{-i2\pi f_b(\beta_j t + \Omega_j)\}$ , and hence we have the result in (iv).

(v) Consider the sampling procedure at  $S_j$ . The sampling impulse train is given by  $\sum_{l=-\infty}^{+\infty} \delta(\beta_j t - lT)$ . Denoting  $t_0$  as the starting point of sampling, and  $T_{ob}$  as the observation interval, we obtain the signal sample sequence  $r_{j,b}[l] = r_{j,b}(lT/\beta_j)$  for  $l = t_0/T : (t_0 + T_{ob})/T$ . We denote  $\bar{r}_{j,b}(t) = \sum_l r_{j,b}[l]\psi_l(t)$ , where  $\psi_l(t) = 1$  for the sample sequence. In general,  $\{\psi_l(t)\}$  constitutes a complete orthonormal basis in the space of band-limited  $\mathcal{L}_2$  functions, for example,  $\psi_l(t) = \sin[\pi(t/T - l)]/[\pi(t/T - l)]\}_{l=-\infty}^{+\infty}$ . The Fourier transform  $\bar{R}_j(\xi)$  is,

$$\begin{aligned} \bar{R}_{j,b}(\xi) &= \sum_l \int r_{j,b}[l]\psi_l(t)e^{-i2\pi\xi t} dt \\ &= \text{rect}(T\xi) \sum_l r_{j,b}[l]e^{-i2\pi\xi lT} = R_{j,b}(\beta_j\xi), \end{aligned}$$

where  $\text{rect}(\cdot)$  denotes the standard rectangular function and acts as an ideal low-pass filter. Therefore, the sampled signal converges in  $\mathcal{L}_2$  to a time-scaled version of the original signal. ■

## APPENDIX B

### PROOF OF THEOREM 1

*Proof:* We first show the signal model  $R_{1,b}(\xi)$  from beacon  $b$  to sensor  $S_1$ . Using Proposition 1, the received signal at  $S_1$  from beacon  $b$  can be obtained by substituting Proposition 1 (ii) and

(iii) into (iv), and we have

$$\begin{aligned}\tilde{R}_{1,b}(\xi) &= \frac{\alpha_{1,b}}{\gamma_{1,b}} \tilde{U}_b \left( \frac{\xi}{\gamma_{1,b}} \right) e^{-i2\pi\xi \frac{\mathcal{T}_{1,b}}{\gamma_{1,b}}} \\ &= \frac{\alpha_{1,b}}{\gamma_{1,b}} \tilde{G}_b \left( \frac{\xi}{\gamma_{1,b}} - f_b \beta_b \right) e^{-i2\pi\xi \frac{\mathcal{T}_{1,b}}{\gamma_{1,b}}} e^{i2\pi f_b \Omega_b},\end{aligned}\quad (31)$$

and hence

$$\begin{aligned}R_{1,b}(\xi) &= \tilde{R}_{1,b}(\xi + f_b \beta_1) e^{-i2\pi f_b \Omega_1} \\ &= \frac{\alpha_{1,b}}{\gamma_{1,b}} \tilde{G}_b \left( \frac{\xi - \Upsilon_{1,b}}{\gamma_{1,b}} \right) e^{-i2\pi\xi \frac{\mathcal{T}_{1,b}}{\gamma_{1,b}}} e^{i2\pi \frac{\Upsilon_{1,b} \mathcal{T}_{1,b}}{\gamma_{1,b}}} e^{i2\pi \varphi_{1,b}} \\ &\propto \tilde{G}_b \left( \frac{\xi - \Upsilon_{1,b}}{\gamma_{1,b}} \right) e^{-i2\pi\xi \frac{\mathcal{T}_{1,b}}{\gamma_{1,b}}},\end{aligned}\quad (32)$$

where  $\varphi_{1,b} = f_b(\Omega_b - \Omega_1 - \beta_b \mathcal{T}_{1,b})$ ,  $\Upsilon_{1,b} = \mathcal{D}_{1,b} \beta_b + f_b(\beta_b - \beta_1)$ . Notice that signals used for the estimation of TDOA and FDOA should be received from the same beacon within the same interval, we assume two sensors make an agreement that they start to collect incoming signals at their local time  $t_0$ . This agreement can be achieved by a prior handshake procedure between two sensors, and we assume  $t_0 = 0$  without loss of generality. Since two sensors are asynchronous, the received signal at  $S_1$  will actually start at the standard time of  $-\Omega_1/\beta_1$  and the collected signal is  $r_{1,b}(t + \Omega_1/\beta_1)$ . Therefore, we further have

$$R_{1,b}(\xi) \propto \tilde{G}_b \left( \frac{\xi - \Upsilon_{1,b}}{\gamma_{1,b}} \right) e^{-i2\pi\xi \frac{\mathcal{T}_{1,b} - \Omega_1/\beta_1}{\gamma_{1,b}}}.\quad (33)$$

Substituting Proposition 1(i) and 1(v) into (33), the result (4) follows easily.

Similarly, we show the signal model  $V_{1,b}(\xi)$  from  $S_2$  to  $S_1$ . Two sensors communicate with each other by transmitting narrowband signals with nominal carrier frequency  $f_0$ . In order to forward its received signal to  $S_1$ ,  $S_2$  shifts the frequency of  $r_{2,b}(t)$  to  $f_0$  using frequency mixer, and obtains the emitted signal, denoted as  $\tilde{u}_{2,b}(t)$ . Using Proposition 1(ii),  $\tilde{u}_{2,b}(t)$  has positive frequency part,

$$\tilde{U}_{2,b}(\xi) = R_{2,b}(\xi - f_0 \beta_2) e^{i2\pi 2f_0 \Omega_2}.\quad (34)$$

Similar to that in (33), the collected signal at  $S_2$  starts at  $-\Omega_2/\beta_2$ , and it follows that

$$R_{2,b}(\xi) \propto \tilde{G}_b \left( \frac{\xi - \Upsilon_{2,b}}{\gamma_{2,b}} \right) e^{-i2\pi\xi \frac{\mathcal{T}_{2,b} - \Omega_2/\beta_2}{\gamma_{2,b}}}.\quad (35)$$

The signal  $\tilde{u}_{2,b}(t)$  is then forwarded to  $S_1$  through the channel  $h_{1,2}(t) = \alpha_{1,2}\delta(\gamma_{1,2}t - \mathcal{T}_{1,2})$ . Using Proposition 1(iii), the received signal at  $S_1$ , denoted as  $\tilde{v}_{1,b}(t)$ , is given by

$$\tilde{V}_{1,b}(\xi) = \frac{\alpha_{1,2}}{\gamma_{1,2}} \tilde{U}_{2,b} \left( \frac{\xi}{\gamma_{1,2}} \right) e^{-i2\pi\xi \frac{\mathcal{T}_{1,2}}{\gamma_{1,2}}}. \quad (36)$$

The received signal  $\tilde{v}_{1,b}(t)$  is then down-converted to baseband using a locally generated carrier wave. From Proposition 1(iv), the down-converted signal at  $S_1$ , denoted as  $v_{1,b}(t)$ , is given by

$$V_{1,b}(\xi) = \tilde{V}_{1,b}(\xi + f_0\beta_1) \exp\{-i2\pi f_0\Omega_1\}. \quad (37)$$

Therefore, substituting (34)–(36) and Proposition 1(i) into (37), it can be shown that

$$\begin{aligned} V_{1,b}(\xi) &= \frac{\alpha_{1,2}\alpha_{2,b}}{\gamma_{1,2}\gamma_{2,b}} \tilde{G}_b \left( \frac{\xi - \Psi_{1,b}}{\gamma_{1,2}\gamma_{2,b}} \right) e^{-i2\pi\xi \frac{\tilde{\Lambda}_{1,b}}{\gamma_{1,2}\gamma_{2,b}}} e^{i2\pi \frac{\Psi_{1,b}\tilde{\Lambda}_{1,b}}{\gamma_{1,2}\gamma_{2,b}}} e^{i2\pi\varphi_1} \\ &\propto G_b \left( \frac{\xi - \Psi_{1,b}}{\beta_b\gamma_{1,2}\gamma_{2,b}} \right) e^{-i2\pi\xi \frac{\beta_b\tilde{\Lambda}_{1,b} - \Omega_b}{\beta_b\gamma_{1,2}\gamma_{2,b}}}, \end{aligned} \quad (38)$$

where  $\varphi_1 = \varphi_{2,b} + \varphi_{1,2} - \Upsilon_{2,b}(\mathcal{T}_{1,2} - \Omega_2/\beta_2)$ ,  $\Psi_{1,b} = [\mathcal{D}_{2,b}\beta_b + f_b(\beta_b - \beta_2)]\gamma_{1,2} + [\mathcal{D}_{1,2}\beta_2 + f_0(\beta_2 - \beta_1)]$ , and  $\tilde{\Lambda}_{1,b} = \gamma_{2,b}\mathcal{T}_{1,2} + \mathcal{T}_{2,b} - \Omega_2/\beta_2$ . Finally from Proposition 1(v), we have the result in (5). ■

## APPENDIX C

### PROOF OF THEOREM 2

*Proof:* We first derive expressions for submatrices of  $\{\mathbf{E}_b, \mathbf{H}_b, \mathbf{K}_b\}_{b=1}^N$ . We summarize the results in the following Lemma 1, whose proof is given in Appendix D.

#### Lemma 1

(i) Suppose Assumption 1 holds, the block matrix  $\mathbf{V}_b$  in (16) is given by

$$\mathbf{V}_b \approx \frac{c^2\mathbf{P}_0\lambda_b}{4} \begin{bmatrix} 1/(1 - \sigma_{\beta_1}^2) & -1/[(1 - \sigma_{\beta_1}^2)(1 - \sigma_{\beta_2}^2)] \\ -1/[(1 - \sigma_{\beta_1}^2)(1 - \sigma_{\beta_2}^2)] & \sigma_{\beta_2}^2/[(1 - \sigma_{\beta_2}^2)^2(1 - 2\sigma_{\beta_2}^2)] \end{bmatrix}. \quad (39)$$

(ii) Suppose Assumption 1 holds, we have

$$\bar{\mathbf{A}}_{E,b} - \bar{\mathbf{B}}_{E,b} \bar{\mathbf{D}}_{E,b}^{-1} \bar{\mathbf{B}}_{E,b}^T \approx \frac{c^2 \mathbf{P}_0}{4} \begin{bmatrix} \lambda_b & -\lambda_b & 0 & 0 \\ -\lambda_b & \lambda_b & 0 & 0 \\ 0 & 0 & \epsilon_b/(1 - \sigma_{\beta_b}^2) & -\epsilon_b/(1 - \sigma_{\beta_b}^2) \\ 0 & 0 & -\epsilon_b/(1 - \sigma_{\beta_b}^2) & \epsilon_b/(1 - \sigma_{\beta_b}^2) \end{bmatrix}, \quad (40)$$

$$\bar{\mathbf{A}}_{H,b} - \bar{\mathbf{B}}_{K,b} \bar{\mathbf{D}}_{E,b}^{-1} \bar{\mathbf{B}}_{K,b}^T \approx \frac{c^2 \mathbf{P}_0}{4} \begin{bmatrix} \lambda_b & 0 \\ 0 & \epsilon_b/(1 - \sigma_{\beta_b}^2) \end{bmatrix}, \quad (41)$$

$$\bar{\mathbf{A}}_{K,b} - \bar{\mathbf{B}}_{K,b} \bar{\mathbf{D}}_{E,b}^{-1} \bar{\mathbf{B}}_{E,b}^T \approx \frac{c^2 \mathbf{P}_0}{4} \begin{bmatrix} -\lambda_b & \lambda_b & 0 & 0 \\ 0 & 0 & -\epsilon_b/(1 - \sigma_{\beta_b}^2) & \epsilon_b/(1 - \sigma_{\beta_b}^2) \end{bmatrix}. \quad (42)$$

Next, we prove Theorem 2 using the above results. It can be seen from (16) that the EFIM for sensor location and velocity is given by

$$\mathbf{F}_{e,s} = \frac{2}{\mathbf{P}_0} \sum_{b \in \mathcal{B}} \mathbf{Q}_b - \left( \frac{2}{c\mathbf{P}_0} \sum_{b \in \mathcal{B}} \mathbf{U}_b \right) \left( \frac{2}{c^2 \mathbf{P}_0} \sum_{b \in \mathcal{B}} \mathbf{V}_b \right)^{-1} \left( \frac{2}{c\mathbf{P}_0} \sum_{b \in \mathcal{B}} \mathbf{U}_b^T \right), \quad (43)$$

which holds if and only if the matrix  $\sum_b \mathbf{V}_b$  is invertible. For the first term in (43), by substituting (40)–(42) into (16), we can obtain

$$\mathbf{Q}_b = \frac{\mathbf{P}_0}{4} \begin{bmatrix} \lambda_b \Phi_b + \epsilon_b \mathbf{P}_b / (1 - \sigma_{\beta_b}^2) & \epsilon_b \Gamma_b / (1 - \sigma_{\beta_b}^2) \\ \epsilon_b \Gamma_b^T / (1 - \sigma_{\beta_b}^2) & \epsilon_b \Pi_b / (1 - \sigma_{\beta_b}^2) \end{bmatrix}, \quad (44)$$

with  $\Phi_b$ ,  $\Pi_b$ ,  $\mathbf{P}_b$ , and  $\Gamma_b$  given in (18), where we have utilized the fact that  $\mathbb{E}\{\beta_m\} = 1$  and  $\mathbb{E}\{1/\beta_m\} = 1/(1 - \sigma_{\beta_m}^2)$  for  $m \in \mathcal{S} \cup \mathcal{B}$  when taking expectations. Similarly, it can be shown that

$$\bar{\mathbf{B}}_{H,b} - \bar{\mathbf{B}}_{K,b} \bar{\mathbf{D}}_{E,b}^{-1} \bar{\mathbf{D}}_{K,b}^T \approx \frac{c^2 \mathbf{P}_0 \lambda_b}{4} \begin{bmatrix} 1/(1 - \sigma_{\beta_1}^2) & -1/(1 - \sigma_{\beta_2}^2) \\ 0 & 0 \end{bmatrix},$$

$$\bar{\mathbf{C}}_{K,b}^T - \bar{\mathbf{B}}_{E,b} \bar{\mathbf{D}}_{E,b}^{-1} \bar{\mathbf{D}}_{K,b}^T \approx \frac{c^2 \mathbf{P}_0 \lambda_b}{4} \begin{bmatrix} -1/(1 - \sigma_{\beta_1}^2) & 1/(1 - \sigma_{\beta_2}^2) \\ 1/(1 - \sigma_{\beta_1}^2) & -1/(1 - \sigma_{\beta_2}^2) \\ 0 & 0 \\ 0 & 0 \end{bmatrix}.$$

Substituting these two terms into (16) and utilizing (39) and Assumption 1, we obtain

$$\left( \frac{2}{c\mathbf{P}_0} \sum_{b \in \mathcal{B}} \mathbf{U}_b \right) \left( \frac{2}{c^2 \mathbf{P}_0} \sum_b \mathbf{V}_b \right)^{-1} \left( \frac{2}{c\mathbf{P}_0} \sum_{b \in \mathcal{B}} \mathbf{U}_b^T \right) \approx \sum_b \frac{\lambda_b}{2} \begin{bmatrix} \mathbb{E} & \mathbf{0} \\ \mathbf{0} & \mathbf{0} \end{bmatrix}, \quad (45)$$

with  $\Xi$  in (18). ■

## APPENDIX D

### PROOF OF LEMMA 1

*Proof:* To begin with, the expressions for  $\{\mathbf{E}_b, \mathbf{H}_b, \mathbf{K}_b\}_{b=1}^N$  are derived using their definitions from (13). For the first term in (13), denoting  $\boldsymbol{\eta}_\mu = [\Delta_{1,b}, \Upsilon_{1,b}]^T$  and utilizing the chain rule of derivative, we have

$$\mathcal{R}e \left\{ \sum_l \frac{\partial \mu_b^*[l]}{\partial \mathbf{y}_m} \left( \frac{\partial \mu_b[l]}{\partial \mathbf{y}_n} \right)^T \right\} = \frac{\partial \boldsymbol{\eta}_\mu}{\partial \mathbf{y}_m} \underbrace{\mathcal{R}e \left\{ \sum_l \frac{\partial \mu_b^*[l]}{\partial \boldsymbol{\eta}_\mu} \frac{\partial \mu_b[l]}{\partial \boldsymbol{\eta}_\mu^T} \right\}}_{\triangleq \mathbf{H}_\mu} \frac{\partial \boldsymbol{\eta}_\mu}{\partial \mathbf{y}_n^T}, \quad (46)$$

where  $m, n \in \{0, b\}$ , and

$$\frac{\partial \mu_b[l]}{\partial \boldsymbol{\eta}_\mu} = e^{-i2\pi\Upsilon_{1,b}t/\beta_1} \begin{bmatrix} \partial g_b(\beta_b/\beta_1 t - \Delta_{1,b})/\partial \Delta_{1,b} \\ -i2\pi t/\beta_1 g_b(\beta_b/\beta_1 t - \Delta_{1,b}) \end{bmatrix}_{t=lT}.$$

Using definitions of  $\mathbf{P}_b$ ,  $\mathbf{T}_b$  and  $\mathbf{W}_b$ , it can be shown that [27]

$$\begin{aligned} \sum_l (2\pi lT)^2 g_b^*(\alpha t - \tau)|_{t=lT} g_b(\alpha t - \tau)|_{t=lT} &= \frac{1}{\alpha^3} 4\pi^2 \mathbf{P}_b \mathbf{T}_b^2, \\ \sum_l \frac{\partial g_b^*(\alpha t - \tau)|_{t=lT}}{\partial \tau} \frac{\partial g_b(\alpha t - \tau)|_{t=lT}}{\partial \tau} &= \frac{1}{\alpha} 4\pi^2 \mathbf{P}_b \mathbf{W}_b^2, \end{aligned}$$

where  $T$  represents the sampling interval, and we have used the approximation of Riemann sum with  $\lim_{T \rightarrow 0} \sum_l g_b(lT)T \approx \int g_b(t)dt$ . It hence follows that

$$\mathbf{H}_\mu = 4\pi^2 \mathbf{P}_b \beta_1 \begin{bmatrix} \mathbf{W}_b^2/\beta_b & 0 \\ 0 & \mathbf{T}_b^2/\beta_b^3 \end{bmatrix},$$

where we have assumed that  $\gamma_{1,2} = 1 + \mathcal{D}_{1,2}/f_0 \approx 1$  and  $\gamma_{j,b} = 1 + \mathcal{D}_{j,b}/f_0 \approx 1$  for  $j = 1, 2$ .

Moreover, recall that  $\Delta_{1,b} = \mathcal{T}_{1,b}\beta_b - \Omega_1\beta_b/\beta_1 - \Omega_b$  and  $\Upsilon_{1,b} = f_b(\gamma_{1,b}\beta_b - \beta_1)$ , we have

$$\frac{\partial \boldsymbol{\eta}_\mu}{\partial \mathbf{y}_0} = \begin{bmatrix} 0 & 0 & -\beta_b/\beta_1 & 0 \\ 0 & 0 & 0 & 0 \end{bmatrix}^T, \quad (47)$$

$$\frac{\partial \boldsymbol{\eta}_\mu}{\partial \mathbf{y}_b} = \begin{bmatrix} \beta_b & 0 & 0 & 0 & \mathcal{T}_{1,b} - \Omega_1/\beta_1 & -1 \\ 0 & 0 & \beta_b & 0 & f_b\gamma_{1,b} & 0 \end{bmatrix}^T. \quad (48)$$

Substituting  $\mathbf{H}_\mu$ , (47), and (48) into (46), we can obtain the expression for the first term in (13).

Similarly, for the second term in (13), denoting  $\boldsymbol{\eta}_\theta = [\Lambda_{1,b}, \Psi_{1,b}]^T$  and utilizing the chain rule of derivative, we have

$$\mathcal{R}e \left\{ \sum_l \frac{\partial \theta_b^*[l]}{\partial \mathbf{y}_m} \left( \frac{\partial \theta_b[l]}{\partial \mathbf{y}_n} \right)^T \right\} = \frac{\partial \boldsymbol{\eta}_\theta}{\partial \mathbf{y}_m} \underbrace{\mathcal{R}e \left\{ \sum_l \frac{\partial \theta_b^*[l]}{\partial \boldsymbol{\eta}_\theta} \frac{\partial \theta_b[l]}{\partial \boldsymbol{\eta}_\theta^T} \right\}}_{\triangleq \mathbf{H}_\theta} \frac{\partial \boldsymbol{\eta}_\theta}{\partial \mathbf{y}_n^T}, \quad (49)$$

where  $m, n \in \{0, b\}$ . It can be shown that  $\mathbf{H}_\theta = \mathbf{H}_\mu$ , and recall that  $\Lambda_{1,b} = \mathcal{T}_{2,b}\beta_b + \mathcal{T}_{1,2}\gamma_{2,b}\beta_b - \Omega_2\beta_b/\beta_2 - \Omega_b$  and  $\Psi_{1,b} = f_b\gamma_{1,2}(\gamma_{2,b}\beta_b - \beta_2) + f_0(\gamma_{1,2}\beta_2 - \beta_1)$ , we have

$$\frac{\partial \boldsymbol{\eta}_\theta}{\partial \mathbf{y}_0} = \begin{bmatrix} \gamma_{2,b}\beta_b & 0 & 0 & -\beta_b/\beta_2 \\ 0 & \beta_b\gamma_{2,b}f_b/f_0 + \beta_2(1 - f_b/f_0) & 0 & 0 \end{bmatrix}^T, \quad (50)$$

$$\frac{\partial \boldsymbol{\eta}_\theta}{\partial \mathbf{y}_b} = \begin{bmatrix} 0 & \beta_b & 0 & \mathcal{T}_{1,2}\beta_b/f_b & \mathcal{T}_{2,b} + \mathcal{T}_{1,2}\gamma_{2,b} - \Omega_2/\beta_2 & -1 \\ 0 & 0 & 0 & \gamma_{1,2}\beta_b & f_b\gamma_{1,2}\gamma_{2,b} & 0 \end{bmatrix}^T. \quad (51)$$

Substituting  $\mathbf{H}_\theta$ , (50), and (51) into (49), we can obtain the expression for the second term in (13).

Therefore, the expressions for  $\{\mathbf{E}_0, \mathbf{E}_b, \mathbf{K}_b\}_{b=1}^N$  follow directly. For example,

$$\mathbf{E}_b = \frac{\partial \boldsymbol{\eta}_\mu}{\partial \mathbf{y}_b} \mathbf{H}_\mu \frac{\partial \boldsymbol{\eta}_\mu}{\partial \mathbf{y}_b^T} + \frac{\partial \boldsymbol{\eta}_\theta}{\partial \mathbf{y}_b} \mathbf{H}_\theta \frac{\partial \boldsymbol{\eta}_\theta}{\partial \mathbf{y}_b^T},$$

substituting the results of (46)-(51) into  $\mathbf{E}_b$  and after some algebra, it can be shown that

$$\mathbf{D}_{E,b} \approx \frac{c^2 \mathbf{P}_0 \lambda_b \beta_1}{2\beta_b} \begin{bmatrix} \delta_1^2 + \delta_2^2 & -(\delta_1 + \delta_2) \\ -(\delta_1 + \delta_2) & 2 \end{bmatrix} + \frac{c^2 \mathbf{P}_0 \epsilon_b \beta_1}{2\beta_b^3} \begin{bmatrix} 2f_b^2 & 0 \\ 0 & 0 \end{bmatrix},$$

where  $\delta_1 = \mathcal{T}_{1,b} - \Omega_1/\beta_1$ ,  $\delta_2 = \mathcal{T}_{2,b} + \mathcal{T}_{1,2}\gamma_{2,b} - \Omega_2/\beta_2$ , and we have approximated  $\gamma_{1,b} = \gamma_{2,b} = \gamma_{1,2} \approx 1$ . The expression for  $\bar{\mathbf{A}}_{E,b} - \bar{\mathbf{B}}_{E,b} \bar{\mathbf{D}}_{E,b}^{-1} \bar{\mathbf{B}}_{E,b}^T$  follows as

$$\bar{\mathbf{A}}_{E,b} - \bar{\mathbf{B}}_{E,b} \bar{\mathbf{D}}_{E,b}^{-1} \bar{\mathbf{B}}_{E,b}^T = \frac{c^2 \mathbf{P}_0}{4} \mathbb{E}_\beta \begin{bmatrix} \lambda_b \beta_b & -\lambda_b \beta_b & 0 & 0 \\ -\lambda_b \beta_b & \lambda_b \beta_b & 0 & 0 \\ 0 & 0 & \epsilon_b/\beta_b & -\epsilon_b/\beta_b \\ 0 & 0 & -\epsilon_b/\beta_b & \epsilon_b/\beta_b \end{bmatrix} - \frac{c^2 \mathbf{P}_0 \lambda_b}{4} \mathbb{E}_\beta \begin{bmatrix} \eta_1^2 & \eta_1 \eta_2 & \zeta_1/f_b & \delta_1/f_b \\ \eta_1 \eta_2 & \eta_2^2 & -\zeta_2/f_b & \delta_2/f_b \\ \zeta_1/f_b & -\zeta_2/f_b & -\Omega_b \zeta_1/f_b^2 & -\Omega_b \delta_1/(\beta_b f_b^2) \\ \delta_1/f_b & \delta_2/f_b & -\Omega_b \delta_1/(\beta_b f_b^2) & 0 \end{bmatrix}, \quad (52)$$

where  $\eta_1 = W_b \delta_1 / (T_b f_b)$ ,  $\eta_2 = W_b \delta_2 / (T_b f_b)$ ,  $\zeta_1 = \Omega_b(1 - \eta_1^2) / \beta_b + \delta_1$ ,  $\zeta_2 = \Omega_b(1 + \eta_1 \eta_2) / \beta_b - \delta_2$ , and we have approximated  $\gamma_{j,b} \approx 1$  for  $j = 1, 2$  and  $\gamma_{1,2} \approx 1$ . When Assumption 1 holds, we have the result in (40). ■

## REFERENCES

- [1] W. P. Tay, J. N. Tsitsiklis, and M. Z. Win, "On the impact of node failures and unreliable communications in dense sensor networks," *IEEE Trans. Signal Process.*, vol. 56, no. 6, pp. 2535–2546, Jun. 2008.
- [2] O. Kreidl and A. Willsky, "An efficient message-passing algorithm for optimizing decentralized detection networks," *IEEE Trans. Autom. Control*, vol. 55, no. 3, pp. 563–578, Mar 2010.
- [3] W. P. Tay, J. N. Tsitsiklis, and M. Z. Win, "Bayesian detection in bounded height tree networks," *IEEE Trans. Signal Process.*, vol. 57, no. 10, pp. 4042–4051, Oct 2009.
- [4] M. Robinson and R. Ghrist, "Topological localization via signals of opportunity," *IEEE Trans. Signal Process.*, vol. 60, no. 5, pp. 2362–2373, 2012.
- [5] V. Moghtadaiee, A. G. Dempster, and S. Lim, "Indoor localization using fm radio signals: A fingerprinting approach," in *Proc. Int Indoor Positioning and Indoor Navigation (IPIN) Conf*, 2011, pp. 1–7.
- [6] M. Bshara, U. Orguner, F. Gustafsson, and L. Van Biesen, "Robust tracking in cellular networks using hmm filters and cell-id measurements," *IEEE Trans. Veh. Technol.*, vol. 60, no. 3, pp. 1016–1024, 2011.
- [7] Y.-S. Chiou, C.-L. Wang, and S.-C. Yeh, "An adaptive location estimator using tracking algorithms for indoor WLANs," *Wirel. Netw.*, vol. 16, no. 7, pp. 1987–2012, Oct. 2010. [Online]. Available: <http://dx.doi.org/10.1007/s11276-010-0240-8>
- [8] W.-S. Ku, K. Sakai, and M.-T. Sun, "The optimal k-covering tag deployment for RFID-based localization," *J. Netw. Comput. Appl.*, vol. 34, no. 3, pp. 914–924, May 2011. [Online]. Available: <http://dx.doi.org/10.1016/j.jnca.2010.04.012>
- [9] A. Yeredor and E. Angel, "Joint TDOA and FDOA estimation: A conditional bound and its use for optimally weighted localization," *IEEE Trans. Signal Process.*, vol. 59, no. 4, pp. 1612–1623, 2011.
- [10] M. Leng and Y.-C. Wu, "Distributed clock synchronization for wireless sensor networks using belief propagation," *IEEE Trans. Signal Process.*, vol. 59, no. 11, pp. 5404–5414, 2011.
- [11] —, "Low-complexity maximum-likelihood estimator for clock synchronization of wireless sensor nodes under exponential delays," *IEEE Trans. Signal Process.*, vol. 59, no. 10, pp. 4860–4870, 2011.
- [12] C.-L. Cheng, F.-R. Chang, and K.-Y. Tu, "Highly accurate real-time GPS carrier phase-disciplined oscillator," *IEEE Trans. Instrum. Meas.*, vol. 54, no. 2, pp. 819–824, 2005.
- [13] F. Cristian, "Probabilistic clock synchronization," *Distributed Computing*, vol. 3, pp. 146–158, 1989.
- [14] T. Li, A. Ekpenyong, and Y.-F. Huang, "A location system using asynchronous distributed sensors," in *Proc. INFOCOM 2004. Twenty-third Annual Joint Conf. of the IEEE Computer and Communications Societies*, vol. 1, 2004.
- [15] —, "Source localization and tracking using distributed asynchronous sensors," *IEEE Trans. Signal Process.*, vol. 54, no. 10, pp. 3991–4003, 2006.
- [16] C. Yan and H. H. Fan, "Asynchronous differential TDOA for non-GPS navigation using signals of opportunity," in *Proc. IEEE Int. Conf. Acoustics, Speech and Signal Processing ICASSP 2008*, 2008, pp. 5312–5315.

- [17] H. C. So, Y. T. Chan, and F. K. W. Chan, "Closed-form formulae for time-difference-of-arrival estimation," *IEEE Trans. Signal Process.*, vol. 56, no. 6, pp. 2614–2620, 2008.
- [18] Y. Shen and M. Win, "Fundamental limits of wideband localization - part I: A general framework," *IEEE Trans. on Information Theory*, vol. 56, no. 10, pp. 4956–4980, oct. 2010.
- [19] B. Sundararaman, U. Buy, and A. D. Kshemkalyani, "Clock synchronization for wireless sensor networks: A survey," *Ad Hoc Networks (Elsevier)*, vol. 3, pp. 281–323, 2005.
- [20] L. L. Lewis, "An introduction to frequency standards," *Proc. IEEE*, vol. 79, no. 7, pp. 927–935, 1991.
- [21] D. Harris and S. Naffziger, "Statistical clock skew modeling with data delay variations," *IEEE Trans. VLSI Syst.*, vol. 9, no. 6, pp. 888–898, 2001.
- [22] R. G. Gallager, *Principles of Digital Communication*. Cambridge : Cambridge University Press, 2008.
- [23] K. L. B. Harry L. Van Trees, Ed., *Bayesian Bounds for Parameter Estimation and Nonlinear Filtering/Tracking*. Wiley-IEEE Press, August, 2007.
- [24] M. Moeneclaey, "On the true and the modified cramer-rao bounds for the estimation of a scalar parameter in the presence of nuisance parameters," *IEEE Trans. Commun.*, vol. 46, no. 11, pp. 1536–1544, 1998.
- [25] F. Gini, R. Reggiannini, and U. Mengali, "The modified cramer-rao bound in vector parameter estimation," *IEEE Trans. Commun.*, vol. 46, no. 1, pp. 52–60, 1998.
- [26] S. M. Kay, *Fundamentals of Statistical Signal Processing: Estimation Theory*. Englewood Cliffs, NJ, 1993.
- [27] F. Hlawatsch and F. Auger, Eds., *Time-Frequency Analysis: Concepts and Methods*. John Wiley & Sons, Inc., 2008.
- [28] S. Stein, "Algorithms for ambiguity function processing," *IEEE Trans. Acoust., Speech, Signal Process.*, vol. 29, no. 3, pp. 588–599, 1981.
- [29] W. H. Foy, "Position-location solutions by Taylor-series estimation," *IEEE Trans. Aerosp. Electron. Syst.*, no. 2, pp. 187–194, 1976.
- [30] J. Smith and J. Abel, "Closed-form least-squares source location estimation from range-difference measurements," *IEEE Trans. Acoust., Speech, Signal Process.*, vol. 35, no. 12, pp. 1661–1669, 1987.
- [31] K. C. Ho and W. Xu, "An accurate algebraic solution for moving source location using TDOA and FDOA measurements," *IEEE Trans. Signal Process.*, vol. 52, no. 9, pp. 2453–2463, 2004.
- [32] K. C. Ho, X. Lu, and L. Kovavisaruch, "Source localization using TDOA and FDOA measurements in the presence of receiver location errors: Analysis and solution," *IEEE Trans. Signal Process.*, vol. 55, no. 2, pp. 684–696, 2007.
- [33] M. Sun and K. C. Ho, "An asymptotically efficient estimator for TDOA and FDOA positioning of multiple disjoint sources in the presence of sensor location uncertainties," *IEEE Trans. Signal Process.*, vol. 59, no. 7, pp. 3434–3440, 2011.
- [34] D. Musicki, R. Kaune, and W. Koch, "Mobile emitter geolocation and tracking using TDOA and FDOA measurements," *IEEE Trans. Signal Process.*, vol. 58, no. 3, pp. 1863–1874, 2010.
- [35] H.-W. Wei, R. Peng, Q. Wan, Z.-X. Chen, and S.-F. Ye, "Multidimensional scaling analysis for passive moving target localization with TDOA and FDOA measurements," *IEEE Trans. Signal Process.*, vol. 58, no. 3, pp. 1677–1688, 2010.